Available online at www.sciencedirect.com

SCIENCE DIRECT®

Coordination Chemistry Reviews 250 (2006) 1210–1233

COORDINATION CHEMISTRY REVIEWS

www.elsevier.com/locate/ccr

Review

Coordination and organometallic compounds and inorganic–organic hybrid crystalline materials for second-order non-linear optics

Elena Cariati, Maddalena Pizzotti, Dominique Roberto, Francesca Tessore, Renato Ugo *

Dipartimento di Chimica Inorganica, Metallorganica e Analitica dell'Università di Milano, Centro di Eccellenza CIMAINA,
and Unità di Ricerca dell'INSTM di Milano via Venezian 21, 20133 Milano, Italy

Received 19 July 2005; accepted 29 September 2005
Available online 3 November 2005

Contents

Abstract

This review concerns the main results obtained in the last few years by our research group at the Dipartimento di Chimica Inorganica Metallorganica e Analitica of the Università degli Studi di Milano, in the field of non-linear optics. After a brief introduction on the basic concepts of non-linear optics (NLO), we report our investigations on the second-order NLO properties of one-dimensional (1D) and 2D coordination and organometallic compounds and hybrid inorganic–organic crystalline materials. Our research has allowed to define some general rules for the design of new appealing NLO compounds and to isolate and identify some new interesting photonic materials.

Keywords: Non-linear optics; Hybrid materials; Organometallic and coordination compounds

---

* Corresponding author. Tel.: +39 02 50314399; fax: +39 02 50314405.
E-mail address: dominique.roberto@unimi.it (R. Ugo).

0010-8545/$ – see front matter © 2005 Elsevier B.V. All rights reserved.
doi:10.1016/j.ccr.2005.09.013

1. Introduction

In the early part of the 1990s, some people in our laboratory made an unusual decision: to leave the area of research on catalysis, both homogeneous and heterogeneous with the exception of surface organometallic chemistry, and to deal "ab initio" with an unknown (for us), but extremely attractive area of research on new materials for photonic and electrooptic applications.

It was not an easy decision since we were quite well known in the area of catalysis while we were absolutely new comers in this specific area of new materials.

In particular, our knowledge on optical physics, on photoemission processes and on the various advanced optical techniques was very limited. However, we were confident in our ability to design complex molecular architectures, either organic or organometallic or of coordination, and in our understanding of the chemistry of the surfaces, layers, etc., at molecular level.

In particular, it appeared to us that in the area of new molecular and crystalline materials for photonic and optoelectronic applications the impact of organometallic and coordination chemistry and the understanding of the role of the nature of metal centers were still limited.

This review describes what we have been able to produce in the last few years after a rather long induction period. Now the scientific production is increasing, since we have at least 10–12 new papers to be published in the next few months in the area of materials for non-linear optics (NLO). We are thus confident that the results and information that we will publish in the near future will integrate and reinforce what reported in this review.

Our research interests are now shifting slowly from the investigation of molecular NLO chromophores to the design and preparation of bulk NLO materials. A similar effort was made in the 1970s when we shifted from homogeneous to heterogeneous catalysis and to surface organometallic chemistry.

Finally, we found extraordinarily the open and easy collaboration of many laboratories and people, experts in the area of electrooptic and photoemission phenomena, which helped us build up our knowledge in this new field and to project and assemble our laboratory of optical physics and photonics.

We feel that such spirit of collaboration is the strength of scientists, which make them unique people. We wish also to thank the Editor for giving us the opportunity to present the results obtained up to now in this adventure.

2. Basic concepts of second-order non-linear optics

2.1. Introduction to second-order non-linear molecular and bulk materials

Non-linear optics represents optical phenomena, caused by the interaction of an oscillating electromagnetic field (light) with specific molecules or bulk materials, with emission of new electromagnetic fields (new light), which differ particularly not only in frequency, but also in phase or other optical properties from the incident ones. In the last decades, the research has been widely developed, due to the possibility to generate potentially interesting new NLO materials for optical or electrooptical devices [1].

When a bulk material experiences an oscillating external electric field (light), there is a perturbation of its electrons and therefore of its polarity, expressed by Eq. (1):

$$\vec{P} = \vec{P}_0 + \vec{P}_{\text{ind}} = \vec{P}_0 + \chi^{(1)}\vec{E} \quad (1)$$

where $\vec{P}_0$ is the intrinsic polarity, $\vec{P}_{\text{ind}}$ is the induced polarization and $\chi^{(1)}$ the electrical susceptibility or linear polarizability tensor. If the applied electric field strength $\vec{E}$ is very high, as it happens in the case of laser pulses, the perturbation is not any more linear with respect to the electric field and the induced polarization is better expressed by a power series according to Eq. (2):

$$\vec{P} = \vec{P}_0 + \chi^{(1)}\vec{E} + \chi^{(2)}\vec{E}^2 + \cdots + \chi^{(n)}\vec{E}^n \quad (2)$$

where $\chi^{(2)}$, $\chi^{(3)}$ and $\chi^{(n)}$, which are tensors, are, respectively, the second-, third- and n-order electrical susceptibilities, which correspond to non-linear responses of the bulk material.

If instead of a bulk material, the applied electromagnetic field is interacting with a molecule, the perturbation is expressed by Eq. (3):

$$\vec{P} = \mu_0 + \alpha\vec{E} + \beta\vec{E}^2 + \gamma\vec{E}^3 + \cdots \quad (3)$$

where μ_0 is the molecular ground state electric dipole moment, α the linear polarizability, β and γ the quadratic and cubic hyperpolarizabilities, respectively. The terms $\beta\vec{E}^2$and $\gamma\vec{E}^3$ correspond to the generation, by a non-linear polarization process, of a second-order and third-order emission of light, with wavelength corresponding to 1/2 or 1/3 of that of the incident light. The intensity of the emission decreases by increasing the order; usually above the third-order it is too low to observe a significant effect. In conclusion, non-linearity is a secondary process of emission of light related to the intensity of the incident light and to the electronic properties controlling the polarizability of molecules or of bulk materials. In particular, both β and $\chi^{(2)}$ vanish in a centrosymmetric structural environment so that, to have a second-order NLO emission, the acentricity requirement must be fulfilled. This is not the case for γ and $\chi^{(3)}$.

In our laboratory, in the last 10 years, we have investigated the design of molecules and crystalline materials with non-linear optical properties both at molecular and at the bulk level, with a particular attention to frequency doubling, called Second Harmonic Generation (SHG). This latter effect is due to the mixing of three waves. Two incident waves with ω frequency interact with the molecule or the bulk material, characterized by a given value of quadratic hyperpolarizability value β or of the second-order electrical susceptibility $\chi^{(2)}$, to produce a new wave, or SH, with frequency 2ω (Fig. 1).

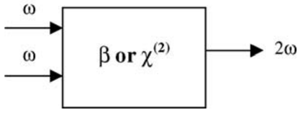

Fig. 1. Second Harmonic Generation (SHG).

To obtain molecular materials displaying significant second-order NLO effects it is necessary to have high values of the molecular quadratic hyperpolarizability β. In 1977, Oudar produced a theoretical interpretation of the electronic origin of β and therefore of the main electronic factors acting on SHG, thus providing a simple model for the design of second-order NLO molecular materials [2]. Since NLO properties are related to the polarizability of the electrons under the effect of the electric field $\vec{E}$ of the light, second-order NLO properties are dependent on electronic transition with high charge-transfer character. Oudar assumed that in asymmetric 1D organic NLO chromophores the second-order NLO response is dominated mainly by one major charge-transfer process, so that it is possible to assume that:

$$\beta_{zzz} = \frac{3}{2h^2c^2}\frac{\nu_{\mathrm{eg}}^2 r_{\mathrm{eg}}^2\,\Delta\mu_{\mathrm{eg}}}{(\nu_{\mathrm{eg}}^2-\nu_{\mathrm{L}}^2)(\nu_{\mathrm{eg}}^2-4\nu_{\mathrm{L}}^2)} \tag{4}$$

where z is the direction of the charge-transfer, ν_{eg} (cm^{-1}) the frequency of the charge-transfer transition, r_{eg} its transition dipole moment, $\Delta\mu_{\mathrm{eg}}$ its difference between the excited state and ground state molecular dipole moment ($\mu_{\mathrm{e}} - \mu_{\mathrm{g}}$) and ν_{L} is the frequency of the incident radiation.

Eq. (4) represents the so-called "two level" model, a simple way to estimate from spectroscopic data the frequency dependent quadratic hyperpolarizability β_{zzz} or β_{CT}, when a single charge-transfer dominates the NLO response. Extrapolation to zero frequency ($\nu_{\mathrm{L}} = 0.0$ eV; $\lambda = \infty$) allows estimation of the static quadratic hyperpolarizability β_0, useful figure of merit to evaluate the basic second-order NLO properties of a molecular material, according to Eq. (5):

$$\beta_0 = \beta_\lambda\left[1-\left(\frac{2\lambda_{\max}}{\lambda}\right)^2\right]\left[1-\left(\frac{\lambda_{\max}}{\lambda}\right)^2\right] \tag{5}$$

where β_λ is the quadratic hyperpolarizability value at λ incident wavelength and $\lambda_{\max}$ is the absorption wavelength of the charge-transfer transition considered.

The molecular quadratic hyperpolarizability β and the second-order susceptibility $\chi^{(2)}$ can be expressed both in the cgs (cm^4 statvolt^{-1} and cm statvolt^{-1} = esu, respectively) or in the SI (C m^3 V^{-2} and m V^{-1}, respectively) unit systems; the conversion from the SI to the cgs system is given by the relation: 10^{-50} C m^3 V^{-2} = 2.694×10^{-30} esu.

The "two level" model allows to evaluate the necessary electronic requirements that a molecule must fulfil in order to show a significant second-order NLO response. It must be non-centrosymmetric, with charge-transfer transitions at relatively low energy and characterized by large $\Delta\mu_{\mathrm{eg}}$ and r_{eg}. This can be achieved in a linear organic chromophore by connecting an electron donor and an electron acceptor group through a π-conjugated polarizable spacer, as it occurs in classical 1D organic dipolar so called push–pull systems (Fig. 2).

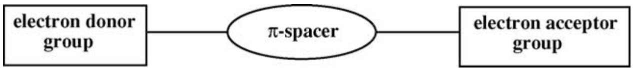

Fig. 2. Scheme of a push–pull chromophore.

In this specific case, the charge-transfer process occurs between the donor and the acceptor group through the polarizable π system, thus producing large $\Delta\mu_{\mathrm{eg}}$ and r_{eg} and a value of $\lambda_{\max}$ controlled by the polarizability of the π system. By increasing polarizability, it shifts to lower energy.

Recently, on the basis of group theoretical and quantum mechanical studies, multipolar systems, such as octupoles, have attracted increasing attention, because it was shown that not only dipolar structures may be of interest for SHG [3]. For molecules belonging to purely octupolar space groups, such as D_3, D_{3h}, T_d, D_2, the vectorial part of the quadratic hyperpolarizability β is cancelled and only the octupolar contribution remains. The advantages of using non-dipolar chromophores include easier non-centrosymmetric arrangements and an improved non-linearity-transparency trade-off.

2.2. Measure of SHG of molecules and bulk materials

To investigate the second-order NLO response of molecular and bulk materials, we have introduced in our laboratory both EFISH and solvatochromic techniques for molecules, and the Kurtz–Perry method for bulk powders. Less frequently, we also used, for molecular measurements in solution, the Hyper-Rayleigh Scattering (HRS) technique, being at the moment not available in our laboratory.

Electric Field Induced Second Harmonic generation (EFISH) [4] is an optical technique, which provides information on the molecular quadratic hyperpolarizability through Eq. (6):

$$\gamma_{\mathrm{EFISH}} = \frac{\mu\beta_\lambda(-2\omega;\omega,\omega)}{5kT} + \gamma(-2\omega;\omega,\omega,0) \tag{6}$$

where $\mu\beta_\lambda(-2\omega;\ \omega,\ \omega)/5\mathrm{kT}$ represents the molecular dipolar orientational contribution and γ $(-2\omega;\ \omega,\ \omega,\ 0)$, a third-order term at frequency ω of the incident light, is the molecular electronic contribution which is negligible for molecules with a limited electronic polarizability. β_λ is the projection along the dipole moment axis of β_{VEC}, the vectorial component of the tensor of the quadratic hyperpolarizability, working with an incident wavelength λ of a pulsed laser. Therefore, in order to obtain the value of β_λ it is necessary to know the ground state dipole moment μ of the molecule. To avoid overestimation of the quadratic hyperpolarizabilty value due to dispersion effects producing resonance enhancements, it is necessary to work with an incident wavelength λ whose second harmonic $\lambda/2$ is far enough from $\lambda_{\max}$ of any absorption of the molecule investigated.

The Hyper-Rayleigh Scattering [3a,5] technique involves the detection of the incoherently scattered second harmonic generated by the molecule in solution under irradiation with a pulsed laser of wavelength λ, leading to the mean value of the $\beta \times \beta$ product. By the analysis of the polarization dependence of the second harmonic signal, which can be evaluated selecting the polarization of the incident and scattered radiation, it is possible to obtain information about the single components of the quadratic hyperpolarizability tensor β. Unlike EFISH, HRS can measure β also for non-dipolar (octupolar) molecules, because it works without a strong applied external electric field.

The solvatochromic method gives access to the evaluation of the quadratic hyperpolarizability along the major charge-transfer direction (β_{CT}), using UV–vis absorption spectra recorded in a series of solvents covering a large dielectric constant and refraction index range and applying Oudar's "two level" model (Eq. (4)). In particular, the solvatochromic method allows to determine $\Delta\mu_{\mathrm{eg}}$, while ν_{eg} and r_{eg} are easily obtained from spectrophotometric measurements, given that the former is the frequency of the charge-transfer transition and the latter is related to its oscillator strength *f*, obtained from the integrated absorption coefficient of the charge-transfer transition band. The value of $\Delta\mu_{\mathrm{eg}}$ can be inferred from the McRae Eq. (7) [6]:

$$(\nu_{\mathrm{eg}})_{\mathrm{s,a}} = (\nu_{\mathrm{eg}})_{\mathrm{g}}^{0} + \delta_{\mathrm{a}} - \left(D + \frac{\mu_{\mathrm{e}}^{2} - \mu_{\mathrm{g}}^{2}}{2hc}\right)\frac{2(n^2-1)}{a^3(2n^2+1)} - \frac{2\mu_{\mathrm{g}}(\mu_{\mathrm{e}} - \mu_{\mathrm{g}})}{hca^3}\left(\frac{\varepsilon - 1}{\varepsilon + 2} - \frac{n^2-1}{n^2+2}\right) \quad (7)$$

where $(\nu_{\mathrm{eg}})_{\mathrm{s,a}}$ and $(\nu_{\mathrm{eg}})_{\mathrm{g}}^{0}$ are, respectively, the frequencies of the absorption maximum in a given solvent s and in the gaseous phase without vibrational excitation; δ_{a} the difference between the vibrational energies of the molecule in the excited and in the ground state; *a* the radius of the cavity (supposed spherical) occupied by the solute molecule in the solvent; ε and *n* the solvent dielectric constant and refractive index and *D* is a term representing the dispersion interactions. When the McRae equation is evaluated for two different solvents, by subtraction of the two expressions a linear equation results, whose intercept is given by Eq. (8):

$$B = -\frac{2\mu_{\mathrm{g}}(\mu_{\mathrm{e}} - \mu_{\mathrm{g}})}{hca^3} \quad (8)$$

This intercept allows the evaluation of $\Delta\mu_{\mathrm{eg}}$ value. The radius *a* of the cavity can be tentatively evaluated from the molecular weight of the compound, using Eq. (9):

$$R = \left(\frac{3M}{4\pi Nd}\right)^{1/3} \quad (9)$$

To have a better indirect estimation of *a*, for fluorescent compounds a methodology has been developed which combines absorption and emission solvatochromisms [6b]. The β_{EFISH} and β_{CT} values can be compared only when the dipole moment axis and the charge-transfer transition are close in direction, while β obtained by HRS measurements cannot be easily compared with β_{EFISH} or β_{CT}.

At the bulk level, the most used method to determine SHG for powder samples is the Kurtz–Perry technique [7]. A powder is irradiated with a pulsed laser and the second harmonic emitted light is collected by a photomultiplier and compared to that of a reference compound such as urea or quartz. Considering that the measured efficiency depends upon bulk electric susceptibility $\chi^{(2)}$, this method gives an indirect evaluation of the order of magnitude of $\chi^{(2)}$. This technique is therefore useful for a first, fast screen of the second-order NLO activity of bulk materials as powders.

3. The effect of coordination to a metal center on the second-order NLO response of mono-, bi- and tri-dentate π-delocalized nitrogen donor push–pull ligands

In the last few years, organometallic and coordination complexes have emerged as interesting molecular chromophores for second-order non-linear optical applications, because they may offer a great diversity of tunable electronic properties by virtue of the metal center [1]. Since the second-order NLO response of various π-delocalized push–pull systems acting as nitrogen donor ligands seems to be enhanced upon coordination to a metal center, we first focused our investigation on the role of the nature of the metal center (electron configuration and oxidation state) and of its coordination sphere on the molecular quadratic hyperpolarizability, β_{λ}, measured by the EFISH method using an incident radiation λ [4], of metal coordinated *para*-substituted pyridines [8], stilbazoles [8–11], phenanthrolines [9] and terpyridines [12,13] (in Fig. 3 are reported the various nitrogen donor ligands investigated). In all our investigations, measure-

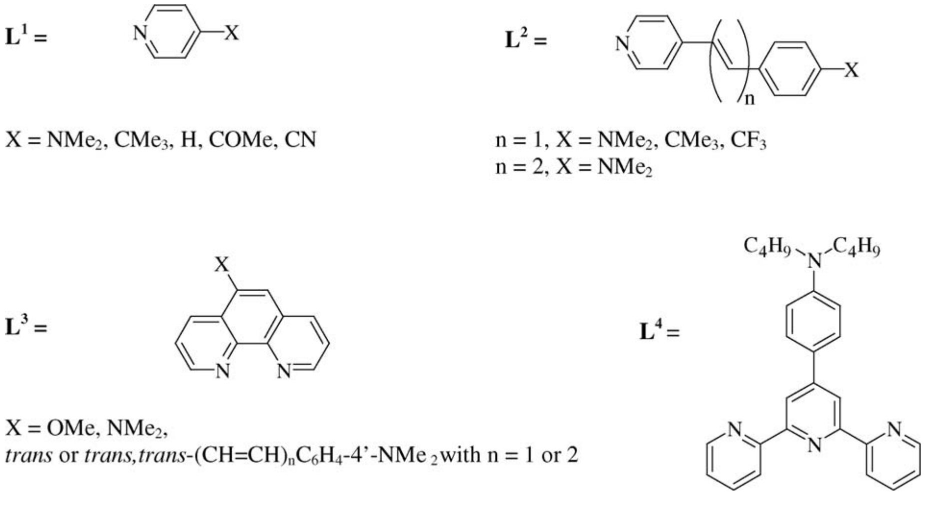

X = NMe_2, CMe_3, H, COMe, CN

n = 1, X = NMe_2, CMe_3, CF_3
n = 2, X = NMe_2

X = OMe, NMe_2,
trans or *trans,trans*-$(CH{=}CH)_nC_6H_4$-4'-NMe_2 with n = 1 or 2

Fig. 3. π-Delocalized nitrogen donor ligands investigated.

ments were carried out in $CHCl_3$ solution with incident radiation of a sufficiently low energy ($\lambda = 1.064$ or 1.34 or 1.907 μm), in order to generate a second harmonic with a wavelength quite far from any significant optical transition so that dispersive resonance enhancement of the EFISH response could be avoided [14].

3.1. The ambivalent donor or acceptor role of the metal acting on the second-order NLO response of push–pull para substituted pyridines and stilbazoles

Initially, we investigated the second-order NLO responses of various organometallic complexes ((**1**)–(**11**); Table 1) such as *cis*-$[M(CO)_2ClL^1]$ (M = Rh, Ir) and *fac*-$[Os(CO)_3Cl_2L^1]$ (see Fig. 3, $L^1 = 4X–C_5H_4N$; X = NMe_2, CMe_3, H, COMe, CN) [8]. EFISH $\beta_{1.06}$ values showed that the metal carbonyl moieties may play, in the excitation processes controlling the second-order NLO response, an ambivalent acceptor or donor role related to their intrinsic softness and to the presence in the pyridine ligand of an electron donor or acceptor group X. For instance, the sign and value of $\beta_{1.06}$ of *cis*-$[M(CO)_2ClL^1]$ (M = Ir(I) ($5d^8$), Rh(I) ($4d^8$)) are dependent upon the nature of X (Table 1):

(i) $\beta > 0$ with strong electron-donating groups (e.g. X = NMe_2: M = Rh, (**1**), $\beta_{1.06}$ 8.7×10^{-30} esu; M = Ir, (**2**), $\beta_{1.06}$ 9×10^{-30} esu);

(ii) β positive but very small with weak electron-donating groups (e.g. X = CMe_3: M = Ir, (**5**), $\beta_{1.06}$ 0.1×10^{-30} esu);

(iii) $\beta < 0$ with strong electron-withdrawing groups (e.g. X = CN: M = Rh, (**9**), $\beta_{1.06}$ -4.3×10^{-30} esu; M = Ir, (**10**), $\beta_{1.06}$ -9×10^{-30} esu).

Table 1
EFISH β values of ligands L^1 and their Rh(I), Ir(I), Os(II) and W(0) complexes

Molecule	X	$\beta_{1.06}$ (10^{-30} esu)[a]	$\beta_{1.91}$ (10^{-30} esu)[b]
L^1	NMe_2	0.07[c]	0.06[c]
cis-$[Rh(CO)_2ClL^1]$ (**1**)	NMe_2	8.7	6.4
cis-$[Ir(CO)_2ClL^1]$ (**2**)	NMe_2	9	6.5
fac-$[Os(CO)_3Cl_2L^1]$ (**3**)	NMe_2	6	4.4
L^1	CMe_3	0.19[d]	0.17[d,e]
cis-$[Rh(CO)_2ClL^1]$ (**4**)	CMe_3	ca. 0	–
cis-$[Ir(CO)_2ClL^1]$ (**5**)	CMe_3	0.1	–
$[W(CO)_5L^1]$	CMe_3	–	−3.4[f]
L^1	H	−0.17[d]	−0.13[d]
cis-$[Rh(CO)_2ClL^1]$ (**6**)	H	2.6	–
fac-$[Os(CO)_3Cl_2L^1]$ (**7**)	H	ca. 0	–
$[W(CO)_5L^1]$	H	–	−4.4[f]
L^1	COMe	−0.029[d]	−0.032[d]
fac-$[Os(CO)_3Cl_2L^1]$ (**8**)	COMe	ca. 2	–
$[W(CO)_5L^1]$	COMe	–	−9.3[f]
L^1	CN	0.33[d]	–
cis-$[Rh(CO)_2ClL^1]$ (**9**)	CN	−4.3	–
cis-$[Ir(CO)_2ClL^1]$ (**10**)	CN	−9	–
fac-$[Os(CO)_3Cl_2L^1]$ (**11**)	CN	ca. 2	–

[a] EFISH values measured in $CHCl_3$ at 1.064 μm.

[b] $\beta_{1.06\,\mu m}$ converted to $\beta_{1.91\,\mu m}$ by the two-level expression (Eq. (5)), unless otherwise stated.

[c] β measured by EFISH at 1.34 μm and converted to $\beta_{1.06\,\mu m}$ or $\beta_{1.91\,\mu m}$ with the two-level expression.

[d] Computed values by using the MNDO-CPHF methodology.

[e] For X = ^{n}Bu instead of CMe_3.

[f] Experimental values from reference [16b]; $\beta_{1.91\,\mu m}$ measured by EFISH in dioxane ($[W(CO)_5L^1]$ (X = ^{n}Bu)), toluene ($[W(CO)_5L^1]$, X = H), or $CHCl_3$ ($[W(CO)_5L^1]$, X = COMe).

The same trend, although less evident, is given by Os(II) ($5d^6$) complexes *fac*-$[Os(CO)_3Cl_2L^1]$ (Table 1). Independently from the strong electron-donating or electron-withdrawing properties of the X group, a very strong enhancement of one or two orders of magnitude of the absolute value of $\beta_{1.06}$ of the pyridine ligands occurs upon coordination.

When X is a strong electron-withdrawing group, the negative sign of $\beta_{1.06}$ is the result of a reduction of the dipole moment upon excitation ($\Delta\mu_{eg} < 0$), according to the two level model [2]. This reduction was first suggested for the related pyridine complexes with zerovalent d^6 metals such as $[M(CO)_5L^1]$ (M = Cr, W; X is an electron-withdrawing group such as CHO or 4′-*trans*-$CH{=}CHC_6H_4CHO$) [15]. The origin of such a reduction of the dipole moment upon excitation is attributed to a dominating effect of a metal-to-ligand charge-transfer (MLCT) transition, which corresponds to an electron shift in the excitation process vectorially opposed to the dipole moment [15].

In our work, we have shown that even a metal carbonyl center with an oxidation state different from zero can act, through the same MLCT excitation process, as an electron-donor toward the pyridine ring. This donation effect becomes less relevant by increasing the oxidation state of the metal, as it can be inferred when comparing the β value of the Os(II) complex with L^1 (X = COMe, (**8**)) with the β value of the related W(0) complex, although both metals have the same $5d^6$ electron configuration (see Table 1).

The metal centers investigated may act also as electron-acceptors toward pyridines substituted with strong electron-donor groups. According to Marks and co-workers [15], EFISH β values of metal complexes with L^1 (X strong donor) are dominated by the red shift of the intraligand $n \rightarrow \pi^*$ charge-transfer (ILCT) transition of the pyridine. This red shift is controlled by the increased electron accepting properties of the metal center which favour the acceptor strength of the π^* orbitals of the pyridine. Therefore, we have shown that we can modulate the NLO response by an increased acceptor strength of the metal centers which is controlled by their oxidation states: e.g. coordination of L^1 (X = NMe_2) to "*cis*-$M(CO)_2Cl$" (M = Rh(I) $4d^8$, (**1**) or Ir(I) $5d^8$, (**2**)) and to "*fac*-$Os(CO)_3Cl_2$" (Os(II) $5d^6$, (**3**)) produces an increase of the EFISH β value 10-fold higher than coordination to the less accepting center "$Cr(CO)_5$" (Cr(0) $3d^6$).

In conclusion, we have shown that by controlling the nature and properties of the metal center it is possible to tune the effects on the second-order NLO response of *para*-substituted pyridines. For instance, the EFISH β value of $[W(CO)_5L^1]$ (X = COMe) is large and negative, even if COMe is not a strong acceptor, because of the good donor properties of the "$W(CO)_5$" fragment [15,16], while for the complex of Os(II) with the same ligand, (**8**), the lower donor properties of the metal center produce an EFISH β value positive although very low (see Table 1). In this latter case, both MLCT and ILCT excitations (corre-

Table 2
Electronic spectra and EFISH β_λ of Rh(I), Ir(I), Os(II), Zn(II) and Pt(II) complexes with ligands L^2

Molecule	X	λ_{max} (nm)[a]	$\mu\beta_0$ (10^{-48} esu)[b]	β_λ (10^{-30} esu)[c]		
				$\beta_{1.06}$	$\beta_{1.34}$	$\beta_{1.91}$
L^2 ($n=1$)	NMe_2	374	137	63	55[d]	35[b]
L^2 ($n=2$)	NMe_2	396	211	124[b]	80	48[b]
L^2 ($n=1$)	CMe_3	362	54	–	–	20
L^2 ($n=1$)	CF_3	303	62	–	–	36
$[Rh(CO)_2ClL^2]$ ($n=1$) (**12**)	NMe_2	421	427	177	111	61[b]
$[Ir(CO)_2ClL^2)]$ ($n=1$) (**13**)	NMe_2	431	402	242[b]	128	67[b]
$[Os(CO)_3Cl_2L^2]$ ($n=1$) (**14**)	NMe_2	435	318[e]	160	83[e]	43[e]
$[Rh(CO)_2ClL^2]$ ($n=2$) (**15**)	NMe_2	442	442	262[b]	131	66[b]
$[Ir(CO)_2ClL^2]$ ($n=2$) (**16**)	NMe_2	449	580	285[b]	135	66[b]
$[Os(CO)_3Cl_2L^2]$ ($n=2$) (**17**)	NMe_2	456	440	260[b]	116	55[b]
$[Rh(COD)ClL^2]$ ($n=1$) (**18**)	NMe_2	397	308	119[b]	77	46[b]
$[Ir(COT)_2ClL^2]$ ($n=1$) (**19**)	NMe_2	413	373	137[b]	82	46[b]
$[Ir(COT)_2ClL^2]$ ($n=2$) (**20**)	NMe_2	430	576	280[b]	152	80[b]
$[Os_3(CO)_{11}L^2]$ ($n=1$) (**21**)	NMe_2	431	441	–	–	65
$[Os_3(CO)_{11}L^2]$ ($n=1$) (**22**)	CMe_3	338 (sh), 376	82	–	–	20
$[Os_3(CO)_{11}L^2]$ ($n=1$) (**23**)	CF_3	312, 385 (sh)	−558	–	–	−78
$[Os_3(CO)_{11}L^2]$ ($n=2$) (**24**)	NMe2	451	633	–	–	98
cis-$[PtCl_2L^2_2]$ ($n=1$) (**25**)[f]	NMe_2	375	–	–	41	–
$[Zn(CH_3CO_2)_2L^2_2]$ ($n=1$) (**26**)[f]	NMe_2	376	–	–	48	–
$[ZnCl_2L^2_2]$ ($n=1$) (**27**)[f]	NMe_2	410	–	–	84	–
$[Zn(CF_3CO_2)_2L^2_2]$ ($n=1$) (**28**)[f]	NMe_2	420	–	–	97	–

[a] Experimental values in $CHCl_3$.

[b] β measured by EFISH at 1.34 μm and converted to β_0 or $\beta_{1.06}$ or $\beta_{1.91}$ with the two-level expression (Eq. (5)).

[c] $\beta_{1.06}$, $\beta_{1.34}$ and $\beta_{1.91}$ measured by EFISH in $CHCl_3$ at 1.064, 1.34 and 1.907 μm, respectively, unless otherwise stated.

[d] β_{CT} at 1.34 μm, obtained from solvatochromic data, is 61, 175 and 230 × 10^{-30} esu for L^2 ($n=1$, X = NMe_2), (**25**) and (**26**), respectively; however by using only the projection of μ_g along the charge-transfer direction β_{CT} is 123 and 132 × 10^{-30} esu for (**25**) and (**26**), respectively.

[e] β measured by EFISH at 1.06 μm and converted to $\beta_{1.34}$ or β_0 or $\beta_{1.91}$ with the two-level expression (Eq. (5), see Section 2).

[f] β, measured by EFISH at 1.34 μm cannot be converted to $\beta_{1.06}$ or β_0 or $\beta_{1.91}$ with the two-level expression (Eq. (5)).

sponding to two vectorially opposed charge-transfer processes) contribute in a similar but opposite extent, while in the much softer W(0) center the MLCT excitation dominates the second-order NLO response, therefore producing negative EFISH β.

In push–pull 1D π-organic chromophores, an increase of the delocalized π-electron bridge between the donor and the acceptor groups can lead to a significant increase in the second-order NLO response [17,18]. We have found on the contrary a buffering of the second-order NLO response, which occurs upon coordination. While by going from L^1 (X = NMe_2) to L^2 (L^2 = 4,4′-*trans* or *trans*,*trans*-$NC_5H_4(CH{=}CH)_nC_6H_4X$, see Fig. 3; $n=1$, X = NMe_2) the enhancement factor of the quadratic hyperpolarizability EFISH β is of the order of 10^3, by going from (**1**)–(**3**) (Table 1) to (**12**)–(**14**) (Table 2) this enhancement factor is about 10 only. Therefore, this kind of metal chromophore, independently from the nature and properties of the metal, cannot display the strong π conjugation length dependence of their quadratic hyperpolarizability typical of organic 1D chromophores [18].

In agreement with this latter statement, the effect due to coordination becomes less and less relevant by increasing the length of the π-delocalized bridge of the push–pull ligand. Thus, coordination to "*cis*-$M(CO)_2Cl$" (M = Rh, Ir) or "*fac*-$Os(CO)_3Cl_2$" of L^2 ($n=1$, 2; X = NMe_2) causes an increase of EFISH β ($\beta_{1.34}$ enhancement factor = 1.5–2.3 for (**12**)–(**17**); Table 2) quite insignificant when compared to the large increase produced on the related pyridine L^1 (X = NMe_2; $\beta_{1.34}$ enhancement factors of ca. 100 for (**1**)–(**3**); Table 1).

Since the balance of the donor–acceptor properties of metal centers seems to be relevant for tuning the second-order NLO response of coordinated pyridines, we investigated also the effect of substitution of CO by olefinic ligands, which should lead to an increase of the electron density on Rh(I) and Ir(I) metal centers and therefore to lower acceptor properties as confirmed by the relatively small red shift of the ILCT transition for olefin Rh(I) (**18**) and Ir(I) (**19**) complexes with L^2 ($n=1$, X = NMe_2; see Table 2). According to lower acceptor properties, EFISH $\beta_{1.34}$ decreases by a factor of ca. 0.7 upon substitution of the carbonyl ligands of *cis*-$[M(CO)_2ClL^2]$ (M = Ir, Rh; $n=1$, X = NMe_2) with cyclooctadiene (COD) or with two cyclooctene ligands (COT) (Table 2). This effect becomes negligible when the length of the π-delocalized electron bridge is increased, as with the ligand L^2 ($n=2$, X = NMe_2; (**20**) Table 2), as expected for a buffering effect.

Interestingly, comparison of EFISH $\beta_{1.91}$ of (**13**) (67 × 10^{-30} esu) with EFISH $\beta_{1.91}$ of 4,4′-*trans*-$NMe_2C_6H_4CH{=}CHC_6H_4NO_2$ (73 × 10^{-30} esu) [18] would suggest that the *cis*-$[Ir(CO)_2Cl]$ moiety behaves as a strong electron-acceptor group similar to the C–NO_2 fragment in the push–pull organic moiety.

Finally, various complexes show $\mu\beta_0$ values between 400 and 600 × 10^{-48} esu, comparable to those of an organic chromophore such as Disperse Red One (*trans*-4,4′-$O_2NC_6H_4N$ =

$NC_6H_4NEt(CH_2CH_2OH)$, $\mu\beta_0 = 500 \times 10^{-48}$ esu) currently proposed for electrooptic polymers [19]. Such excellent $\mu\beta_0$ values are due to two electronically related factors: an enhancement in the dipole moment μ generated by coordination to the metal center acting in the ground state always as an acceptor, and in parallel an enhancement of β_0 due, for instance, to a significant red shift of the ligand ILCT transition.

3.2. *The effect of coordination to a metal cluster carbonyl core on the second-order NLO response of 4,4′-trans or trans,trans-$NC_5H_4(CH{=}CH)_nC_6H_4X$ (L^2; n = 1, X = NMe_2, CMe_3, CF_3; n = 2, X = NMe_2)*

Although metal nanoparticles are known to display interesting NLO properties, due to the "softness" of their electron structure, nothing was reported on the interaction of push–pull organic chromophores like those based on *para*-substituted stilbazoles with potentially electron rich polynuclear metallic fragments such as "soft" metal carbonyl clusters. Therefore, we investigated the effect of coordination of the *para*-substituted stilbazoles L^2 ($n = 1$, X = NMe_2, CMe_3, CF_3; $n = 2$, X = NMe_2) to a metal carbonyl cluster core such as "$Os_3(CO)_{11}$" in order to investigate if the cluster moiety introduces additional relevant effects (Table 2, (**21**)–(**24**)) [20].

The ILCT $n \rightarrow \pi^*$ transition of push–pull organic ligands, containing an electron donor NMe_2 group, is red-shifted upon coordination ((**21**), (**24**): $\Delta\lambda_{max} = 55$–57 nm); the amount of the shift suggests unexpectedly an acceptor strenght of the "$Os_3(CO)_{11}$" core comparable to that of Os(II) or Ir(I) metal centers such as "*fac*-$Os(CO)_3Cl_2$" and "*cis*-$Ir(CO)_2Cl$" [8] (Table 2). On the contrary, the absorption band attributed to a $\pi \rightarrow \pi^*$ ligand transition of L^2 ($n = 1$, X = CMe_3) is only slightly red-shifted upon coordination ((**22**) $\Delta\lambda_{max} = 14$ nm) and also the absorption spectrum of L^2 ($n = 1$, X = CF_3) displays upon coordination (**23**) a slightly red-shifted $\pi \rightarrow \pi^*$ internal transition with respect to the free ligand ($\Delta\lambda_{max} = 9$ nm), but together with a shoulder at about 385 nm attributed to a MLCT transition from the "$Os_3(CO)_{11}$" core to the π^* levels of the stilbazole ligand bearing the electron-withdrawing CF_3 group.

These observations, together with similar trends of the increase of the dipole moment upon coordination, would suggest that the interaction of these push–pull ligands with a cluster core of a zero valent metal, is quite similar to that with M(I) (M = Rh, Ir) or Os(II) carbonyl complexes.

As expected, if the osmium cluster core does not play a relevant additional effect, ligands with a donor group (NMe_2) display by coordination (compounds (**21**) and (**24**)) an enhancement of EFISH $\beta_{1.91}$, which decreases by increasing the length of the π-delocalized bridge. Besides, coordination of a ligand with a poor electron donor like the *t*-butyl group (compound (**22**)) does not produce a relevant effect on EFISH $\beta_{1.91}$, while coordination of a ligand carrying an electron acceptor group (compound (**23**)) produces a negative sign of EFISH $\beta_{1.91}$ (Table 2), since in this latter case the second-order NLO response is dominated by the MLCT transition. This latter result confirms that the "$Os_3(CO)_{11}$" core behaves also as an electron donor by a MLCT process.

β_0 values, calculated by the two level approach [2] suggest that the "$Os_3(CO)_{11}$" core displays acceptor properties closer to Os(II) in "*fac*-$Os(CO)_3Cl_2$" than to W(0) in "$W(CO)_5$". Coordination of L^2 ($n = 2$; X = NMe_2) to the "$Os_3(CO)_{11}$" core induces a perturbation leading to higher β_0 value than coordination to "*cis*-$M(CO)_2Cl$" (M = Rh(I), Ir(I)) or to "*fac*-$Os(CO)_3Cl_2$" [8]. There are no second-order NLO measurements of W(0), Rh(I), Ir(I), Ru(II) and Os(II) carbonyl complexes bearing the ligand L^2 ($n = 1$, X = CF_3), but a comparison of $\beta_{1.91}$ of its complex with "$Os_3(CO)_{11}$" (**23**) with $\beta_{1.91}$ of $[W(CO)_5L^2]$ ($n = 1$, X = NO_2) [16b] (respectively, -78 and -20×10^{-30} esu) suggests that the potentially electron rich "$Os_3(CO)_{11}$" cluster core behaves as a very good donor to the π^* levels of L^2 ($n = 1$; X = CF_3).

In summary, our investigation reached the conclusion that a zerovalent trimeric cluster core such as "$Os_3(CO)_{11}$" shows an ambivalent "acceptor–donor" behavior more relevant than that of monomeric metal carbonyl moieties such as "$M(CO)_5$" (M = W(0)), "*cis*-$M(CO)_2Cl$" (M = Rh(I), Ir(I)) and "*fac*-$Os(CO)_3Cl_2$", but it does not introduce additional effects due only to the cluster electrons.

3.3. *The role of the metal and of the ancillary ligands on the second-order NLO response of π delocalized nitrogen donor push–pull ligands*

The remarkable increase of EFISH $\beta_{1.34}$ of the flexible chelating ligand 4-(*p*-dibutylaminostyryl)-4′-methyl-2,2′-bipyridine upon coordination to the Zn(II) Lewis acids [21] (enhancement with respect to the free ligand of about 10 times) prompted us to investigate the effect of coordination on the second-order NLO response of structurally related push–pull ligands, such as the non-chelating stilbazole L^2 ($n = 1$, X = NMe_2), in order to define the role of chelation and of more rigid chelating ligands 5-X-1,10-phenanthrolines (L^3, X = donor group such as OMe, NMe_2, *trans*-$CH{=}CHC_6H_4$-4′-NMe_2 and *trans,trans*-$(CH{=}CH)_2C_6H_4$-4′-NMe_2; see Fig. 3) in order to define the role of ligand rigidity [9]. The choice of position 5 of the 1,10-phenanthroline ring was based on a preliminary MNDO-CPHF theoretical investigation for the identification of the best position (2, 3, 4 or 5) on the 1,10-phenanthroline ligand, for the substituent "*trans*-$CH{=}CHC_6H_4NMe_2$" in order to produce a push–pull phenantroline ligand with significant second-order NLO response.

As shown in Table 2, the EFISH $\beta_{1.34}$ value of L^2 ($n = 1$, X = NMe_2) is almost not affected by coordination to the relatively soft "*cis*-$PtCl_2$" moiety and strangely enough to the "$Zn(CH_3CO_2)_2$" less soft Lewis acid, in agreement with the irrelevant red shift of the ILCT transition upon coordination of L^2 to "*cis*-$PtCl_2$" ((**25**): $\Delta\lambda_{max} = 1$ nm) and "$Zn(CH_3CO_2)_2$" ((**26**): $\Delta\lambda_{max} = 2$ nm). However, this red shift increases significantly upon coordination to harder "ZnY_2" (Y = Cl (**27**), CF_3CO_2 (**28**)) Lewis acids, with a β enhancement factor (β EF) function of the ancillary Y ligands (for (**27**) and (**28**), β EF = 1.5 and 1.8, respectively), in agreement with a large red shift of the ILCT transition ($\Delta\lambda_{max} = 36$ and 46 nm for (**27**) and (**28**), respectively). Chelation seems to have a positive effect on the second-order NLO response because the $\mu\beta_{1.34}$

value (1420×10^{-48} esu) reported for [$ZnCl_2$(4,4′-bis(*trans*-CH=CHC_6H_4-4′-NBu_2)-2,2′-bipyridine)] [22] is much higher than that of the structurally related non-chelated complex with two stilbazole L^2 ligands (**27**) (706×10^{-48} esu). This is due to the more planar arrangement of the chelated ligand and therefore to a stronger perturbation of the π^* orbitals and therefore to a more facile ILCT $n \rightarrow \pi^*$ transition.

The lack of a significant increase upon coordination to "*cis*-$PtCl_2$" or "$Zn(CH_3CO_2)_2$" of the quadratic hyperpolarizability of L^2 ($n = 1$, $X = NMe_2$; (**25**) and (**26**)) was confirmed by a solvatochromic study (see footnotes in Table 2) [9]. As above mentioned (Section 2), the quadratic hyperpolarizability β_{CT}, obtained by solvatochromic measurements, can be compared to EFISH β only when the charge-transfer transition involved in the NLO response is close in direction to the axis of the dipole moment [6b]. Thus, for square planar Pt(II) (**25**) and tetrahedral Zn(II) (**26**) complexes, β_{CT} at 1.34 μm (175 and 230×10^{-30} esu, respectively) results to be much higher than EFISH $\beta_{1.34}$ (41 and 48×10^{-30} esu, respectively) because the dipole moment axis is not coincident with the direction of the ILCT transition located on the stilbazole ligand. Of course in the free stilbazole ligand, which shows a good agreement between β_{CT} at 1.34 μm and EFISH $\beta_{1.34}$, the dipole moment axis and the ILCT direction are coincident. According to this observation, when only the component of the dipole moment along the ILCT charge-transfer direction is considered for both "$Zn(CH_3CO_2)_2$" and "*cis*-$PtCl_2$" complexes, the resulting value of β_{CT} (123 and 132×10^{-30} esu, respectively) becomes only slightly higher than twice that of the stilbazole ligand itself, confirming the irrelevant perturbation of the free ligand upon coordination to "$Zn(CH_3CO_2)_2$" or "*cis*-$PtCl_2$", already suggested by the irrelevant red shift of the ILCT transition in both complexes and the comparable value between EFISH $\beta_{1.34}$ of (**25**), (**26**) and that of the free stilbazole ligand [9].

Since the increase of the quadratic hyperpolarizability of L^2 ($n = 1$, $X = NMe_2$) is clearly a function of the ancillary Y ligands which tune the acceptor properties of the Zn(II) center ($CH_3CO_2 < Cl < CF_3CO_2$), we investigated the second-order NLO response of [$Zn(CF_3SO_3)_2{L^2}_2$] ($X = NMe_2$; $n = 1$ (**29**), $n = 2$ (**30**)) complexes, since $CF_3SO_3^-$ is a very weak donor ancillary ligand (Fig. 4).

At concentrations higher than 1×10^{-4}M, the value of EFISH $\beta_{1.91}$ is increased by a factor of ca. three to six times with respect to that of related acetate (**26**) or trifluoroacetate (**28**) complexes, in agreement with a much higher Lewis acidity of the Zn(II) center (Table 2). However, at concentrations lower than ca. 10^{-4} M, the $\beta_{1.91}$ value of these triflate complexes increases abruptly by decreasing concentration, up to huge values, while this effect is not observed for the related acetate or trifluoroacetate complexes (Fig. 4).

This behavior was attributed to an increased concentration (although very low because EFISH measurements are still possible) of the ion pair with the cation $[Zn(CF_3SO_3)L_2^2]^+$ ($n = 1$ or 2, $X = NMe_2$), produced by solvolysis of the triflate ligand, as confirmed by electrical conductivity measurements, which evidenced a sharp conductivity increase at concentrations below 10^{-4} M for triflate complexes (Fig. 5) [10].

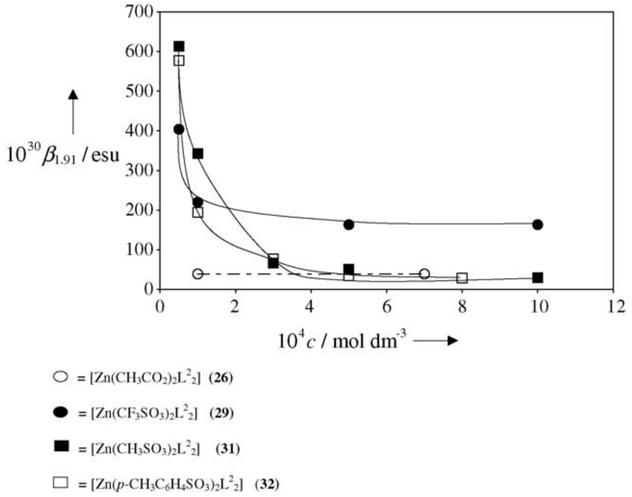

Fig. 4. Dependence of $\beta_{1.91}$ upon concentration c for various [$ZnY_2L_2^2$] complexes ($n = 1$, $X = NMe_2$) (ref. [10], with copyright permission). (○) [$Zn(CH_3CO_2)_2L_2^2$] (**26**); (●) [$Zn(CF_3SO_3)_2L_2^2$] (**29**); (■) [$Zn(CH_3SO_3)_2L_2^2$] (**31**); (□) [Zn(*p*-$CH_3C_6H_4SO_3)_2L_2^2$] (**32**).

By working at relatively high concentration (>3×10^{-4} M) with other less electron-withdrawing non-fluorinated sulfonate ligands, such as methanesulfonate or *para*-toluenesulfonate, the second-order NLO response is unexpectedly comparable to that of the related complexes with acetate or trifluoroacetate as ancillary ligands, despite the significantly higher red shift of the ILCT transition of the push–pull L^2 ($n = 1$, $X = NMe_2$) ligand. Such unexpected low value of the second-order NLO response of Zn(II) complexes of L^2 with methanesulfonate (**31**) or *para*-toluenesulfonate (**32**) as ancillary ligands was attributed to a

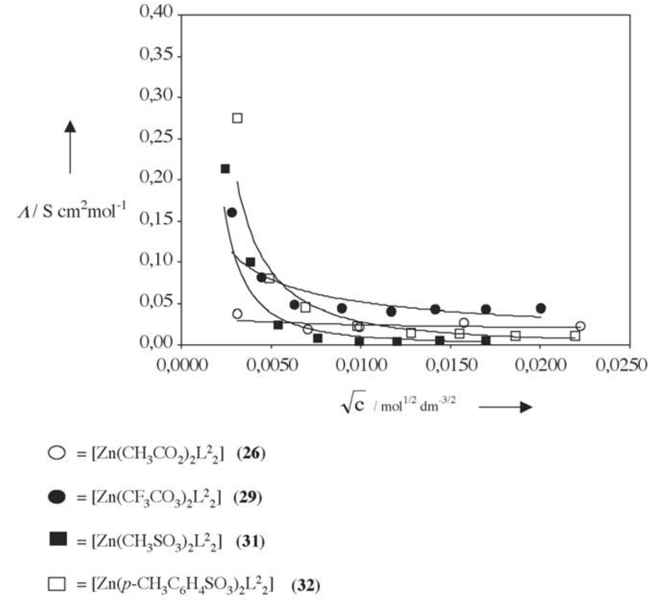

Fig. 5. Dependence, in $CHCl_3$ at 298 K, of molar conductance Λ of various [$ZnY_2L_2^2$] complexes ($n = 1$, $X = NMe_2$) vs. the square root of the concentration c (ref. [10], with copyright permission). (○) [$Zn(CH_3CO_2)_2L_2^2$] (**26**); (●) [$Zn(CF_3SO_3)_2L_2^2$] (**29**); (■) [$Zn(CH_3SO_3)_2L_2^2$] (**31**); (□) [Zn(*p*-$CH_3C_6H_4SO_3)_2L_2^2$] (**32**).

process of association which occurs at high concentration, originated by their rather high dipole moment. This process of association does not play a relevant role on the NLO response of complexes with the triflate ancillary ligand, since for these latter conductivity evidence supports already some solvolysis, even at high concentration. However, when working at diluted conditions (less than 10^{-4} M), all the sulfonate Zn(II) complexes behave in the same way with a huge increase of $\beta_{1.91}$ (Fig. 4). Therefore, ionic dissociation by dilution in anhydrous $CHCl_3$ remains a typical behavior of all Zn(II) complexes carrying an ancillary sulfonate ligand, independently from their electron-withdrawing character and therefore of their nucleophilic properties.

Interestingly, with this investigation on Zn(II) complexes with sulfonated ancillary ligands, we have evidenced for the first time that the effect of the concentration *should not* be neglected when investigating the second-order molecular NLO properties.

We have also investigated the second-order NLO response of some phenanthroline complexes $[M(CH_3CO_2)_2L^3]$ (M = Zn, X = OMe (**33**) NMe_2 (**34**), *trans*-CH=CHC_6H_4-4′-NMe_2 (**35**) and *trans*,*trans*-$(CH{=}CH)_2C_6H_4$-4′-NMe_2 (**36**); M = Cd, X = *trans*-CH=CHC_6H_4-4′-NMe_2 (**37**)) [9].

EFISH $\beta_{1.34}$ values of L^3 ligands increase with the electron-donating strength of the X substituent, and as expected, more significantly with the introduction of a π-conjugated electron bridge linking the NMe_2 group to the phenanthroline ring, in agreement with the increased red shift of λ_{max} of the ILCT $n \rightarrow \pi^*$ transition (Table 3) major origin of the second-order NLO response, with the phenanthroline π^* orbitals acting as electron acceptors. However, although the red shift of the ILCT of L^3 (X = *trans*-CH=CHC_6H_4-4′-NMe_2) upon coordination to "$Cd(CH_3CO_2)_2$" (**37**) or "$Zn(CH_3CO_2)_2$" (**35**) is comparable, this is not reflected by the EFISH $\beta_{1.34}$ value which is almost unaffected by coordination to the relatively soft "$Cd(CH_3CO_2)_2$" acid whereas it is significantly increased by coordination to the harder "$Zn(CH_3CO_2)_2$" acid (Table 3). The enhancement factor of EFISH $\beta_{1.34}$ ($\beta_{1.34}$ EF) upon coordination of 5-X-1,10-phenanthrolines to "$Zn(CH_3CO_2)_2$" is higher for the better donor group (X = NMe_2, (**34**): β $EF_{1.34} = 4.6$) than for a lower donor group (X = OMe, (**33**): β $EF_{1.34} = 3.2$). It becomes less and less relevant by increasing the length of the π-delocalized bridge between the donor group NMe_2 and the phenanthroline moiety ((**35**), (**36**)), as it occurs with 4-X-pyridines [8], but the EFISH $\beta_{1.34}$ value of L^3 (X = NMe_2; 7.2×10^{-30} esu) is much higher (by a factor of 10^2) than that of L^1 (X = NMe_2; 0.07×10^{-30} esu), as expected for the larger π-conjugated electron network of the phenanthroline system which acts as a better π^* acceptor in the $n \rightarrow \pi^*$ ILCT transition than the pyridine ring.

The second-order NLO response of the various phenanthrolines and related complexes was also investigated by the solvatochromic method. A very good correspondence between β_{CT} at 1.34 μm and EFISH $\beta_{1.34}$ was found (Table 3), suggesting a satisfactory coincidence of the direction of the ILCT charge-transfer and of the dipole moment axis. The solvatochromic investigation allowed also a more subtle investigation of the origin of the second-order NLO response [9]. When the donor group NMe_2 is not directly linked to the phenanthroline ring (L^3 with X = *trans*- or *trans*,*trans*-$(CH{=}CH)_nC_6H_4$-4′-NMe_2; $n = 1$ or 2) the appreciable increase of β_{CT} upon coordination to "$Zn(CH_3CO_2)_2$" is due to a high oscillator strength and to the low energy of the ILCT transition, rather than to an increase of the $\Delta\mu_{eg}$, which on the contrary decreases upon coordination, while when NMe_2 is directly linked to the phenanthroline ring (X = NMe_2), the relevant enhancement of β_{CT} is mainly due to a large increase of $\Delta\mu_{eg}$. In the Cd(II) complex (**37**), the lack of increase of EFISH $\beta_{1.34}$ by coordination despite the red shift of the ILCT transition is explained by the too small decrease of the energy of this latter transition and by the relatively small increase of its oscillator strength which do not compensate the unexpected high decrease of $\Delta\mu_{eg}$, thus, finally producing in total an irrelevant enhancement of β_{CT} [9].

Table 3
Electronic spectra, EFISH $\beta_{1.34}$ in $CHCl_3$ and β_{CT} of ligands L^3 and their complexes with "$Zn(CH_3CO_2)_2$" and "$Cd(CH_3CO_2)_2$"

Molecule	X	λ_{max} nm[a,b]	$\mu\beta_0$ (10^{-30} esu)[c]	EFISH $\beta_{1.34}$[a] (β_{CT})[d] (10^{-30}esu)
L^3	OMe	272	9.6	4.0[e]
L^3	NMe_2	328	20	7.2 (9.3)
L^3	*trans*-CH=CHC_6H_4-4′-NMe_2	371	127	41 (58)
L^3	*trans*-$(CH{=}CH)_2C_6H_4$-4′-NMe_2	399	215	75
$[Zn(CH_3CO_2)_2L^3]$ (**33**)	OMe	284	74	13
$[Zn(CH_3CO_2)_2L^3]$ (**34**)	NMe_2	344	175	33 (32)
$[Zn(CH_3CO_2)_2L^3]$ (**35**)	*trans*-CH=CHC_6H_4-4′-NMe_2	419	338	77 (71)
$[Zn(CH_3CO_2)_2L^3)]$ (**36**)	*trans*-$(CH{=}CH)_2C_6H_4$-4′-NMe_2	432	450	112
$[Cd(CH_3CO_2)_2L^3)]$ (**37**)	*trans*-CH=CHC_6H_4-4′-NMe_2	411	202	46
4-(*trans*-CH=CHC_6H_4-4′-NBu_2)-4′-CH_3-2,2′-bipyridine[f]		388	41	14
$[Zn(CH_3CO_2)_2$(4-(*trans*-CH=CHC_6H_4-4′-NBu_2)-4′-CH_3-2,2′-bipyridine)][f]		447	450	116

[a] Experimental values in $CHCl_3$.

[b] λ_{max} (ILCT) mainly involved in the NLO response [9].

[c] β measured by EFISH at 1.34 μm and converted to β_0 with the two-level expression (Eq. (5)).

[d] Obtained from solvatochromic data at 1.34 μm [9].

[e] A similar $\beta_{1.34}$ value (3.7×10^{-30} esu) is obtained by carrying out the EFISH measurement at 1.06 μm and converting it to $\beta_{1.34}$ with the two-level expression (Eq. (5)).

[f] Ref. [21].

Table 4
Electronic spectra, EFISH $\beta_{1.34}$ and $\beta_{CT,1.34}$ of ligand L^4 and its complexes with Zn(II), Ru(III) or Ir(III)

Molecule	λ_{max} nm[a]	$\lambda_{max (em)}$ nm[a,b]	EFISH $\beta_{1.34}$ (β_0)[c] 10^{-30} esu	$\beta_{1.34}$ EF[d]	f[a,e]	$\Delta\mu_{eg}$ D[f]	$\beta_{CT,\ 1.34}$ 10^{-30} esu[g]
L^4	360[h]	449	22 (15)	–	0.40	8.0	43
$ZnCl_2L^4$ (**38**)	425[h]	503	67 (36)	3.0	0.33	10.8	98
$Zn(CF_3CO_2)_2L^4$ (**39**)	427[h]	512	88 (47)	4.0	0.34	8.2	79
$IrCl_3L^4$ (**40**)	465[h,i]	624	−109	5.0	0.81	−0.1	−4
	533[j]				0.31	−2.9	−79
							–
							−83
$Ru(CF_3CO_2)_3L^4$ (**41**)	416[h]	590	−70	3.2	0.15	12.7	48
	508[k]				0.20	5.4	75
	911[k]				0.04	15.8	−208
							–
							−85

[a] In $CHCl_3$ solution.

[b] λ_{max} of the emission.

[c] In parentheses β_0 calculated by the two-level approach (Eq. (5)).

[d] $\beta_{1.34}$ EF is $\beta_{1.34}$ enhancement factor that is $\beta_{1.34}$ complex/$\beta_{1.34}$ free terpyridine.

[e] f is the oscillator strength obtained from the integrated absorption coefficient.

[f] $\Delta\mu_{eg}$ is the difference between excited and ground state molecular dipole moments, obtained from solvatochromic data; see ref. [6].

[g] Quadratic hyperpolarizability tensor along the charge-transfer direction.

[h] Attributed to the ILCT of the ligand.

[i] Due to the anomalous high intensity and the unexpected slightly negative $\Delta\mu_{eg}$, an expected MLCT transition is located under the strong ILCT transition.

[j] Tentatively assigned to MLCT.

[k] Tentatively assigned to LMCT.

We finally investigated the effect on the second-order NLO response of coordination to various metal ions in relatively high oxidation state of polychelated push–pull nitrogen donor π-delocalized ligands carrying an electron donor substituent such as 4′-(C_6H_4-*p*-NBu_2)-2, 2′: 6′, 2″-terpyridine (L^4, complexes (**38**)–(**41**); see Fig. 3) [12]. In this latter case, since the free ligand is probably in a transoid configuration, as suggested by its low dipole moment, coordination produces a double effect due to both chelation and perturbation of the electronic π system.

In all complexes, the ILCT transition at about 416–465 nm is red-shifted ($\Delta\lambda_{max}$ = 56–105 nm) with respect to that of the free ligand, due to the increased acceptor properties of its π^* orbitals upon chelation (Table 4) [15]. The enhanced EFISH $\beta_{1.34}$ value of the terpyridine L^4 upon coordination to "ZnY_2" ((**38**), (**39**)) remains positive as it occurs in all the Zn(II) complexes with similar nitrogen donor push–pull chelated ligands [9,21]. The enhancement factor is higher for the more electron-withdrawing ancillary ligand CF_3CO_2. However, upon coordination of L^4 to $IrCl_3$ or $Ru(CF_3CO_2)_3$ (compounds (**40**) and (**41**)), the absolute value of EFISH $\beta_{1.34}$ increases significantly, in agreement with a relevant red shift of the ILCT transition, but the sign becomes negative (Table 4).

Therefore, our investigation has shown for the first time that different metal centers, which all behave as strong Lewis acids according to the red shift of the ILCT transition of the ligand, can influence not only the absolute value but also the sign of the quadratic hyperpolarizability of a nitrogen donor π-delocalized push–pull ligand bearing a strong electron-donor group. A solvatochromic investigation confirmed that also β_{CT} is positive for Zn(II) complexes ((**38**) and (**39**)) and negative for Ir(III) and Ru(III) complexes ((**40**) and (**41**); Table 4) and has been a way to define the electronic origin of these effects. The large enhancement of the quadratic hyperpolarizability of L^4 upon coordination to Zn(II) is due, as in other Zn(II) complexes [9,21], to both a significant red shift of the ILCT transition and a positive $\Delta\mu_{eg}$ (Table 4). However, for the Ir(III) complex (**40**) the second-order NLO response is not dominated by the ligand ILCT transition only but there is a contribution of two other bands at 533 nm and ca. 465 nm tentatively assigned to MLCT (metal-to-ligand charge-transfer) transitions according to literature [23] and to their negative $\Delta\mu_{eg}$ (Table 4).

Besides, in the terpyridine Ru(III) complex (**41**), the negative sign of β originates from the high contribution to the second-order NLO response of an absorption band at 911 nm, in opposition to the positive contribution of another absorption band at 508 nm and to the expected positive contribution of the ILCT transition at 416 nm (Table 4). The new transitions, both characterized by a positive value of $\Delta\mu_{eg}$ (Table 4), were tentatively assigned to LMCT (ligand to metal charge-transfer) transitions [24,25]. However, the absorption at 911 nm is located at lower energy then the second harmonic (λ = 670 nm) and therefore produces naturally a negative contribution to the quadratic hyperpolarizability when this latter is measured at an incident wavelength of 1.34 μm. Recently, we confirmed by a Time-Dependent Density Functional Theory (TD-DFT) investigation that the band at 911 nm can be attributed to a LMCT transition, whereas the absorption band at 508 nm is not originated by a single transition, but is composed by three transitions of mixed character with a predominant ILCT character and some component of MLCT character [13].

In conclusion, with a series of strongly connected investigations we have shown that a metal center can perturb in a very efficient and sometimes predictable way the second-order NLO response of π delocalized nitrogen donor push–pull ligands. The fine-tuning can be achieved by working on the nature of the metal center, its oxidation state and its coordination sphere.

4. Organometallic counterparts of push–pull aromatic chromophores for non-linear optics: push–pull heteronuclear bimetallic complexes with pyrazine and *trans*-1,2-bis(4-pyridyl)ethylene as linkers

The body of investigations reported in Section 3 prompted us [26] to investigate the second-order NLO response of some asymmetric heteronuclear push–pull bimetallic complexes with pyrazine (pyz) (complexes (**42**)–(**44**)) and *trans*-1,2-bis(4-pyridyl)ethylene (BPE) (complexes (**45**)–(**47**)) as π polarizable linkers, between the "$W(CO)_5$" fragment (acting as donor group) [15] and "*cis*-$Rh(CO)_2Cl$", "*cis*-$Re(CO)_4Cl$" and BF_3 (acting as acceptor groups) [8,27,28] (Table 5). These molecular systems can be considered as organometallic counterparts of classical 1D push–pull organic chromophores, where the donor or acceptor groups are organometallic moieties or metal complexes. The second-order NLO response of these bimetallic complexes was initially compared to that of related monomeric $[W(CO)_5L]$ complexes (L = *para*-substituted pyridine or *trans*-stilbazole para substituted with strong organic acceptor groups) and then to that of classic organic push–pull chromophores.

Coordination of "$(CO)_5W(pyz)$" to "BF_3" and "$Rh(CO)_2Cl$" to generate a bimetallic push–pull system leads to an increase of the absolute value of the quadratic hyperpolarizability EFISH $\beta_{1.91}$, dominated by the MLCT ($W \rightarrow \pi_L^*$) transition of the "$W(CO)_5(pyz)$" moiety (Table 5), red-shifted by coordination of the free nitrogen atom of pyrazine to "*cis*-$Rh(CO)_2Cl$" (**44**), "*cis*-$Re(CO)_4Cl$" (**43**), or BF_3 (**42**), acting as acceptor groups. This latter interaction stabilizes the π_L^* acceptor orbitals of the pyrazine bridge. In the case of (**42**), the charge-transfer is in the direction of the ground state dipole moment leading to a positive quadratic hyperpolarizability, while in the case of (**44**) the charge-transfer is in the opposite direction, leading to a negative response. For (**43**), the second-order NLO response becomes negligible probably because the electronic structure $5d^6$ of Re(I) in "*cis*-$Re(CO)_4Cl$" is similar to that of W(0) in "$W(CO)_5$", so that we have not really a push–pull system. Recent theoretical TD-DFT calculations have confirmed both the above discussed origin and trends of second-order NLO response [26,29].

The second-order NLO response of monomeric and heteronuclear dimeric complexes with BPE as ligand or linker confirms that it is dominated by the MLCT ($W \rightarrow \pi_L^*$) transition of the "$W(CO)_5BPE$" moiety [15]. In heteronuclear dimeric complexes, the negative quadratic hyperpolarizability remains negative in agreement with the significant negative $\Delta\mu_{eg}$ value of the MLCT ($W \rightarrow \pi_L^*$) transition of $[(CO)_5W(BPE)BF_3]$. Its value increase is due to the enhancement of acceptor properties of the π_L^* orbitals of BPE upon coordination, as supported by the red shift of the MLCT transition [26].

It is worth mentioning that the introduction of an electron acceptor nitro group in the *para* position of *trans*-stilbazole in $[W(CO)_5L^2]$ complexes (L^2 with X = H or NO_2) produces an increase of the quadratic hyperpolarizability from −5.6 to -20×10^{-30} esu [16b], comparable to that from −7 to -49×10^{-30} esu induced by coordination of BF_3 to the free nitrogen atom of $[W(CO)_5BPE]$. However, coordination of $[W(CO)_5BPE]$ to BF_3 produces an inversion of the sign of the ground state dipole moment [26], which does not occur by substitution of X = H with X = NO_2 in $[W(CO)_5L^2]$ complexes [16b].

Table 5
EFISH $\beta_{1.91}$ and $\Delta\mu_{eg}$ for some pyrazine and BPE complexes

Molecule[a]	Complex no.	$\beta_{1.91}$	$\Delta\mu_{eg}$
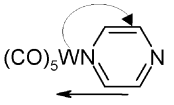		−6[b,c]	<0
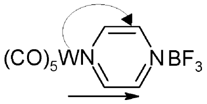	(**42**)	38[d]	>0
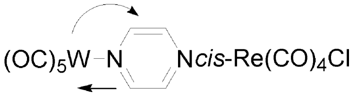	(**43**)	≈0[b,d]	≈0
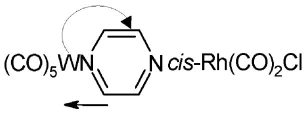	(**44**)	−33[d] −28[b]	<0
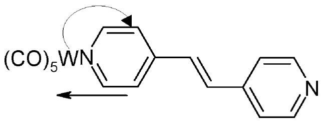		−7[b]	<0
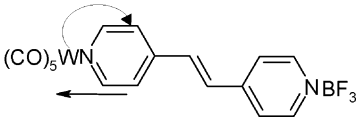	(**45**)	−49[d]	<0
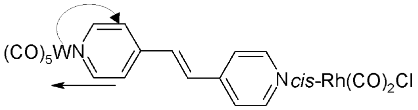	(**46**)	−41[b]	<0
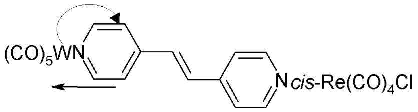	(**47**)	−79[d]	<0
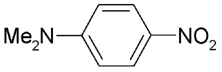		12[c]	–
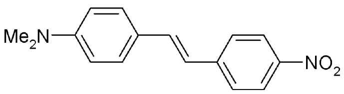		73[c]	–

[a] The straight arrows give the direction of the charge distribution in the ground state (by convention opposite the dipole moment vector).

[b] Experimental values obtained by means of the EFISH technique, using $CHCl_3$ as solvent.

[c] Ref. [16b].

[d] Experimental values obtained by means of the solvatochromic methodology, with determination of the cavity radius a from structural data.

When compared to structurally related push–pull aromatic 1D chromophores there are some relevant differences. The MLCT process ($W \rightarrow \pi_L^*$), which is the major origin of the second-order NLO response in the asymmetric organometallic push–pull chromophores investigated [1c,f], remains localized on the part of the π bridge close to the push donor center (e.g. "$W(CO)_5$") even after coordination at the other end of the bridge of an inorganic or organometallic center acting as pull electron acceptor center. Therefore, the electronic process dominating the second-order NLO response never assumes a MMCT (metal to metal charge-transfer) character, with the charge-transfer process involving both the donor and acceptor inorganic centers via the polarizable bridge as it occurs between the donor and acceptor groups in structurally related classical push–pull aromatic 1D chromophores [18a].

It follows that when the distance between the "$W(CO)_5$" donor group and the acceptor group (for instance, "*cis*-$Rh(CO)_2Cl$" or BF_3) is small, such as when pyrazine is the bridge, the perturbation on the pull group and therefore on the MLCT ($W \rightarrow \pi_L^*$) is strong enough to generate a change of the sign of the second-order NLO response, while the absolute value of the quadratic polarizability assumes values higher than in structurally related classical *para*-substituted push–pull benzenic chromophores [18]. However, this effect becomes less relevant by increasing the length of the π delocalized bridge between the push and pull groups, as when BPE is the bridge, while in structurally related organic π-delocalized push–pull 1D chromophores the second-order NLO response increases by increasing the length of the π-delocalized bridge [18a].

Therefore, we have organometallic push–pull chromophores with a much larger second-order NLO response when the length of the bridge is limited (compare the value of 38×10^{-30} esu of $[(CO)_5W(pyz)BF_3]$ (**42**) with 12×10^{-30} esu of *para*-nitro dimethyl aniline) [16b], while it is less significant and of different sign when the length of the bridge increases (compare the value of -49×10^{-30} esu of $[(CO)_5W(BPE)BF_3]$ (**45**) with 73×10^{-30} esu of *trans*-4-dimethylamino, 4′ nitro stilbene) [18a].

In a second time, in order to enhance the second-order NLO response of this kind of bimetallic heteronuclear chromophores with the pyrazine bridge, we tried to increase the donor properties of the "$W(CO)_5$" moiety by substitution of two carbonyls with a 1,10-phenanthroline (phen) [30]. However, the "$(CO)_3W(phen)$" moiety is a too weak acceptor and a relatively strong base, therefore, when $[(CO)_3(phen)Wpyz]$ interacts with soft acidic fragments like "*cis*-$M(CO)_2Cl$" (M = Rh(I), Ir(I)), pyrazine is lost, whereas "$(CO)_3W(phen)$" interacts as a base, producing a new class of heteronuclear bimetallic complexes of the type [(phen)$(CO)_3$W *cis*-$M(CO)_2Cl$] (M = Rh(I) (**48**), Ir(I) (**49**)) and [(phen)$(CO)_3$W *fac*-$M(CO)_3Cl_2$] (M = Ru(II) (**50**), Os(II) (**51**)). All these new heteronuclear bimetallic complexes show in their electronic spectra a new solvatochromic absorption band at around 385–450 nm in addition to the MLCT ($W \rightarrow \pi_{phen}^*$) absorption band typical of $[W(CO)_3(phen)L]$ complexes (L = CO, pyz, CH_3CN) and an increase, in comparison to $[W(CO)_4(phen)]$ ($\beta_{1.91} = -13 \times 10^{-30}$ esu), of the absolute value of the negative second-order NLO response ($\beta_{1.91} = -31.7 \times 10^{-30}$, -25.8×10^{-30}, -76×10^{-30} and -75.6×10^{-30} esu, for (**48**), (**49**), (**50**) and (**51**), respectively). The increase of the absolute value is probably due to an additional negative contribution of an absorption band at 385–450 nm, with a MLCT character, as confirmed by a solvatochromic investigation [30].

5. Inorganic–organic hybrid crystalline materials

Requirements for non-linear optical materials to be applicable in specific devices include not only significant SHG but also mechanical, thermal and chemical properties. Molecular NLO chromophores such as organic, organometallic or coordination compounds must be transformed into layers, films or crystals, where they are highly ordered in a non-centrosymmetric way, to produce bulk materials, which must be characterized by the above properties. This microscopic order can be induced by different techniques or may spontaneously be obtained by mechanism of self-organization as, for instance, during a crystallization process. This latter aspect was investigated in our laboratory in the new area of hybrid inorganic–organic crystalline NLO materials.

5.1. New ionic layered compounds of Cu(I)

Although the design of organic molecules with large quadratic hyperpolarizabilities β is now quite well studied, little is known about the criteria needed in order to obtain a non-centrosymmetric crystalline packing arrangement, *conditio sine qua non*, to get a non-zero second-order non-linear optical response for crystalline materials [31]. A large molecular dipole, which favours high β values, is actually a potential driving force toward centric crystals. In salts, however, Coulombic interactions could overwhelm the deleterious dipole–dipole interactions and allow an asymmetric assembly of polar ionic moieties. This concept, proposed by Meredith [32], was successfully applied by Marder et al. [17e] and resulted in one of the most active (1000 times urea) second harmonic generator organic crystalline materials ever reported, that is [*trans*-4-(4-dimethylaminostyryl)-1-methylpyridinium][*para*-toluenesulfonate], hereafter [$DAMS^+$][PTS].

Following this approach, interest for new crystalline materials with very high SHG has been recently focused on inorganic–organic hybrids, capable to merge the advantages of the organic NLO chromophores (appreciable NLO response speed and intensity in a wide spectral range, straightforward synthetic approach) to those of an inorganic network (chemical, thermal and mechanical stabilities). High second-order NLO responses have been reported to occur in highly ordered hybrid inorganic–organic salts, such as the intercalated species [$DAMS^+$]-MPS_3 (M = Mn, Cd, Zn) [33,34] and the layered mixed oxalates [$DAMS^+$-like cations][$M^{II}Cr^{III}(C_2O_4)_3$] (M = Mn, Fe, Co, Ni, Cu) [35] or the species [$DAMS^+$]$PbI_3 \cdot 2DMSO$ [36]. In all these materials, the very high SHG is originated by a specific high ordered arrangement of the organic chromophore [$DAMS^+$] within the crystalline structure.

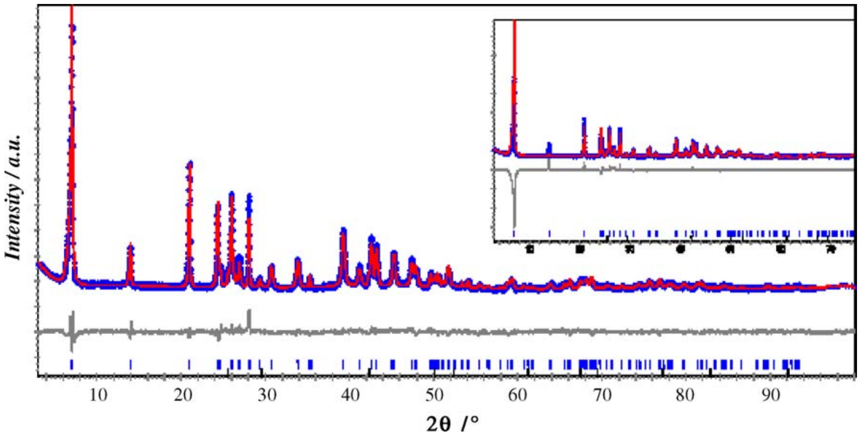

Fig. 6. XRPD pattern of $[DAMS^+][Cu_5I_6]$ (ref. [37], with copyright permission).

When working in this research area, we have isolated and structurally characterized a new layered salt of formula $[DAMS^+][Cu_5I_6]$ (**52**) which shows a huge SHG efficiency (same order of magnitude of $[DAMS^+]$[PTS] working with an incident 1.907 μm non-resonant wavelength) [37]. We were unable to prepare suitable single crystals, consequently we resorted to ab initio X-ray powder diffraction (XRPD) methods to retrieve its structure [38]. The characterization via powder diffraction data was possible because the inorganic host structural features could be retraced to a "unique" crystallographic model, to which the specific nature of the organic guest imparts secondary modifications, since powders of (**52**) show a very simple XRPD pattern (Fig. 6).

The structural motif consists of polymeric CuI slabs stacked along the trigonal axis (Fig. 7). The slabs are formed by two parallel, slightly corrugated sheets. $[DAMS^+]$ cations fill the empty space within the slabs and are organized in J-type (or Scheibe) aggregates [39]. In fact, as in $[DAMS^+]$-MPS_3 intercalates [32,33], $[DAMS^+][Cu_5I_6]$ shows, as KBr pellets (Fig. 8), the superposition of two absorption bands: a broad and strong band centered around 510 nm, resembling that of solid $[DAMS^+]$I (Fig. 8), and a strong, narrow signal at 580 nm, indicative of J-aggregates of the $[DAMS^+]$ cation. These aggregates, according to the original formulation by Scheibe, consist of densely packed domains of chromophores characterized by a peculiar, more narrow, and red-shifted visible absorption band, with respect to the parent monomeric chromophore. We concluded thus that the very high SHG is due to this self-arrangement, within two host slabs, of the intercalated $[DAMS^+]$ cations, which are edge-on oriented (the interslab spacing being 12.75 Å), dipole ordered and densely packed (as J-aggregates).

Trying to rationalize the origin of the self-organization process we tentatively suggested that it is the guest ($[DAMS^+]$) that drives the microscopic interlayer dipole ordering and therefore the overall crystal order. The factor controlling the formation of macroscopic ordering is the intrinsic polarity of the "first" $[DAMS^+]$ guest layer that imparts a definite "order" to the host vacancies, which therefore determines the orientation of the next guest add-layer.

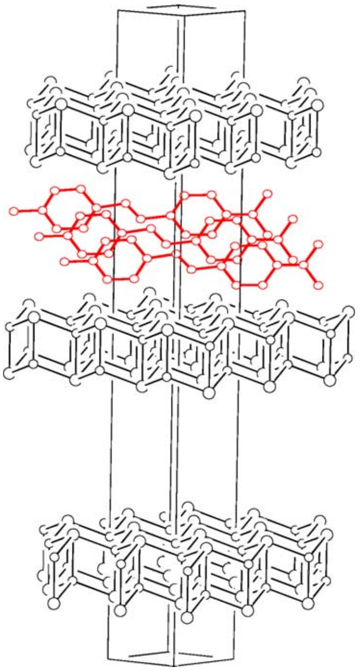

Fig. 7. The wavy and Cu-defective slabs of the Cu_5I_6 host lattice. Each $[DAMS^+]$ cation extends over three adjacent cells (ref. [37], with copyright permission).

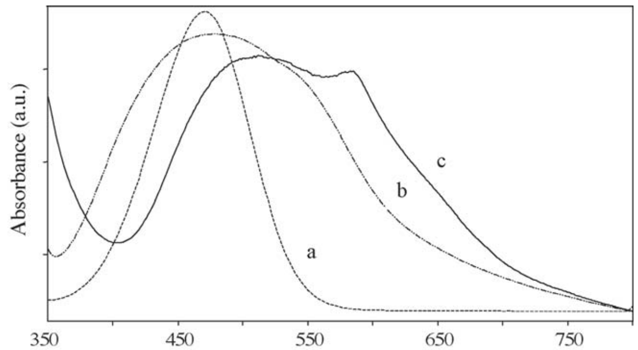

Fig. 8. Electronic absorption spectra; (a) $[DAMS^+]$I in CH_3CN; (b) $[DAMS^+]$I in KBr; (c) $[DAMS^+][Cu_5I_6]$ in KBr.

5.2. Polymeric coordination compounds of Cu(I)

Among the inorganic–organic hybrid materials, the adducts between Group 11 metal halides (MX, with X = Cl, Br or I) and mono-hapto Lewis bases (such as pyridines) with a donor nitrogen atom (L) are particularly intriguing for both the variety of structural motifs and the related optical emission displayed [40]. Actually, structural motifs such as [CuX(L)] monomers [41], $[CuX(L)_2]_2$ dimers [42], $[CuX(L)]_4$ tetramers [43], $[CuX(L)]_n$ single-stranded ‘zig-zag chain’ [44] and double-stranded ‘stair’ polymers [44a,d,45] have been reported. Photoluminescence properties have been systematically analyzed only for CuI tetramers [46]: their solid state, room temperature low energy (LE) yellow emission (centered around 580–625 nm) has been interpreted as a decay from a triplet ‘cluster centered’ ($^3CC^*$) excited state. The latter involves the I_4 and Cu_4 tetrahedra and has mixed halide-to-metal charge-transfer ($^3XMCT^*$) and $d_{Cu} \rightarrow (s,p)_{Cu}$ character. Copper···copper distances lower than the sum of the van der Waals radii (2.80 Å) have been invariably found and considered as an indirect proof of the $d_{Cu} \rightarrow (s,p)_{Cu}$ contribution, for which a significant overlap among the orbitals of the Cu_4 core is required. At variance, the solid state room temperature emissive behavior of polymers has been investigated just for a few double-stranded ‘stairs’ (namely $[CuI(pyridine)]_n$, $[CuI(3\text{-methylpyridine})]_n$ [47] and $[CuI(4\text{-methylpyridine})]_n$ [47]). For the high energy (HE) blue emissions observed (respectively, centered at 437, 454 and 437 nm), a decay from a triplet halide-to-ligand charge-transfer ($^3XLCT^*$) excited state has been invoked. In this latter case any contribution from metal-delocalized orbitals has been discarded on the basis of copper···copper distances greater than 2.80 Å.

Despite these significant charge-transfer processes, no systematic investigations have been performed on the solid-state second-order NLO responses of oligomeric and polymeric CuX/L adducts. Only recently, we have reported [48] the syntheses, the crystal structures, the emissive and solid-state second-order NLO properties of two new non-centrosymmetric ‘chain’ and ‘stair’ polymeric adducts between CuI and 4-acetylpyridine ((**53a**)–(**53b**)). In compound (**53a**), with [Cu:I:acpy] = [1:1:1] stoichiometry, the [CuI(acpy)] asymmetric units arrange in polymeric $[CuI(acpy)]_n$ double-stranded ‘stairs’ (Fig. 9); in (**53b**), with [Cu:I:acpy] = [1:1:2] stoichiometry, copper and iodine atoms are arranged alternately along ‘zig-zag single-stranded chains’ (Fig. 10) originating the rare $[CuX(L)_2]_n$ motif, encountered previously just in $[CuCl(HNA)_2]_n$ (HNA = nicotinic acid) [49].

(**53a**) shows a single intense emission centered at 612 nm, rather red-shifted with respect to the $^3XLCT^*$ emission of the structurally related $[CuI(pyridine)]_n$ ‘stair’, centered at 437 nm. Such bathochromic shift, unexpectedly pronounced to be completely attributed to the energetic stabilization of the π^*_L levels of the organic ligand, did not allow to discriminate between a decay from a $^3XLCT^*$ or a $^3MLCT^*$ excited state at the origin of the emissive behavior. (**53b**) shows an emission band centered around 700 nm. We suggested that the excited state responsible for this emission is $^3XLCT^*$ in character, in analogy to the few studies on the photoluminescence of CuI/L ‘stairs’ adducts (Table 6).

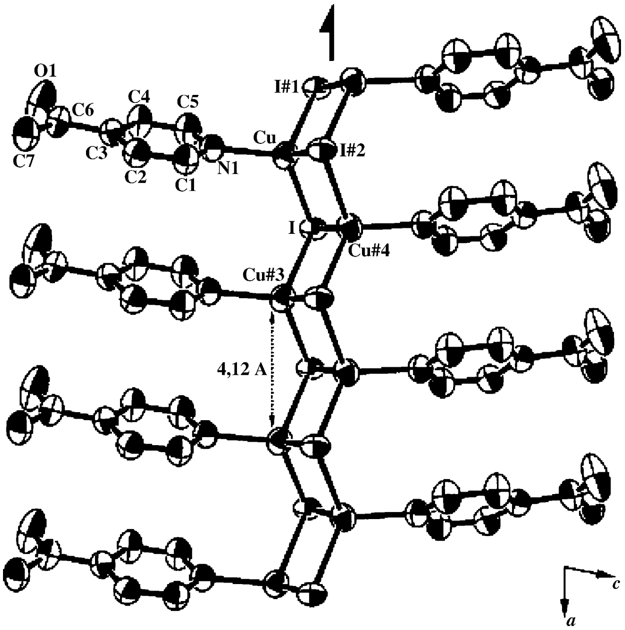

Fig. 9. Representation (with 50% probability, Ortep) of the double-stranded stair, structural motif for (**53a**) (ref. [48], with copyright permission).

Both crystalline materials proved to be second harmonic generators as powders: SHG efficiencies about 1 and 14 times that of urea have been recorded for (**53a**) and (**53b**), respectively. To rationalize such a different second-order NLO behavior, we carried out a comparison of their experimental SHG’s to the

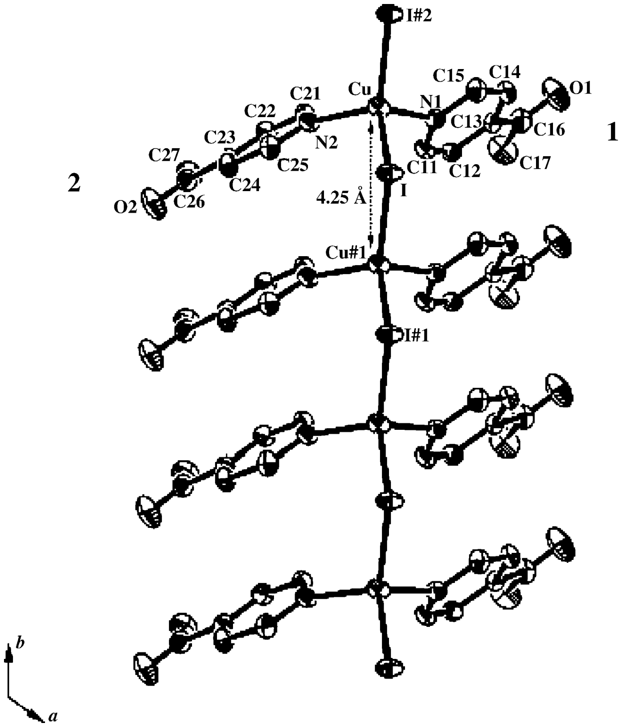

Fig. 10. Representation (with 50% probability, Ortep) of the zig-zag single-stranded chain, structural motif for (**53b**) (ref. [48], with copyright permission).

Table 6
Halide, ligand, stoichiometry, structural motif, photoluminescence emission maximum and powder efficiency in second harmonic generation for compounds (**53**)–(**59**)

	X	L[a]	Stoichiometry	Motif	$\lambda_{max(em)}$ (nm)	SHG
(**53a**)	I	acpy	$[CuX(L)]_n$	'Stair'	612	1[b]
(**53b**)	I	acpy	$[CuX(L)_2]_n$	'Chain'	ca. 700	14[b]
(**54**)	Cl	quin	$[CuX(L)]_n$	'Stair'	602	Negligible[c]
(**55**)	Cl	quind	$[CuX(L)]_n$	'Chain'	590	2.3[c]
(**56**)	Br	py	$[CuX(L)]_n$	'Stair'	509	Negligible[c]
(**57**)	Br	trimeth	$[CuX(L)]_n$	'Chain'	418, 536	22.5[c]
(**58**)	Br	quind	$[CuX(L)]_n$	'Chain'	645	7.5[c]
(**59**)	I	trimeth	$[CuX(L)]_n$	'Chain'	443, 535	45.0[c]

[a] py, pyridine; acpy, 4-acetilpyridine; quin, quinoline; quind, 2-methylquinoline; trimeth, 2,4,6-trimethylpyridine.
[b] Measured at an incident wavelength of 1.907 μm with respect to urea.
[c] Measured at an incident wavelength of 1.064 μm with respect to quartz.

phase-matchable components of b_{eff} using Zyss' formulas [50]. This resulted in b_{eff}(**53a**) of about $0.050\beta_{\mathrm{CT}}$(**53a**) and b_{eff}(**53b**) of about $0.300\beta_{\mathrm{CT}}$(**53b**). This assuming that the origin of the second-order NLO response is a metal-to-ligand charge-transfer ^{3}MLCT* process and that the molecular quadratic hyperpolarizability along the metal-to-ligand axis β_{CT} is almost identical in (**53a**) and (**53b**) (an acceptable approximation considering that M and L are in both materials the same). Comparison of the experimental SHG(**53b**)/SHG(**53a**) ratio (about 14) to the calculated b_{eff}(**53b**)/b_{eff}(**53a**) one (about 6) produced an indirect evidence of the inadequacy of a ^{3}MLCT* process alone to explain the electronic origin of the second-order NLO response for (**53a**) and (**53b**). Thus, in order to attempt a rationalization of both second-order NLO activities and emissions of this kind of polymeric inorganic–organic hybrid Cu(I) crystalline materials, we investigated the emissive and second-order NLO properties of some structurally related non-centrosymmetric $[CuX(L)]_n$ 'chains' and 'stairs' adducts with a series of pseudo-aromatic ligand with a nitrogen donor atom (L), namely $[CuCl(quinoline)]_n$ (**54**) [45f], $[CuCl(2\text{-methylquinoline})]_n$ (**55**) [44c], $[CuBr(pyridine)]_n$ (**56**) [45d], $[CuBr(2,4,6\text{-trimethylpyridine})]_n$ (**57**) [44c], $[CuBr(2\text{-methylquinoline})]_n$ (**58**) [44c] and $[CuI(2,4,6\text{-trimethylpyridine})]_n$ (**59**) [44c].

The 'stairs' $[CuBr(pyridine)]_n$ (**56**) and $[CuCl(quinoline)]_n$ (**54**) show a broad emission centered at 509 and 602 nm, respectively, quite red-shifted with respect to that at 437 nm of $[CuI(pyridine)]_n$. Given both the structural motif and the large Cu···Cu distances (3.07 and 2.91 Å, for (**54**) and (**56**), respectively), it seemed reasonable, in both cases, to discard any participation of a cluster type metal-delocalized orbitals. In addition, being the wavelength of the emission modulated by the nature of X, an influence of the halide on the charge-transfer processes controlling the emissions of either $[CuI(pyridine)]_n$, or (**54**) and (**56**) appeared plausible, so that the decay processes could be originated from a ^{3}XLCT* excited state involving the halide.

The emissive behavior of the 'chain' structures was found to be more complex. The two structurally related 'chains' $[CuCl(2\text{-methylquinoline})]_n$ (**55**) and $[CuBr(2\text{-methylquinoline})]_n$ (**58**) showed solid state emission bands at 590 and 645 nm, respectively. The Cu···Cu contacts (3.80 and 3.90 Å for (**55**) and (**58**), respectively) seemed to preclude, even in this case, a 'metal cluster centered' contribution to the emission process, however, a well founded discrimination between the ^{3}XLCT* and ^{3}MLCT* processes is not possible, although in favour of the first, we noted that, L being the same, the wavelength of the emission for (**55**) and (**58**) varies with the nature of X. Finally, two distinct emissions were observed for the two structurally related 'chains' $[CuBr(2,4,6\text{-trimethylpyridine})]_n$ (**57**) and $[CuI(2,4,6\text{-trimethylpyridine})]_n$ (**59**) ($\lambda_{\mathrm{em}}^{\max} = 418$ and 536 nm, 'structured', and 443 and 535 nm, respectively). Their low energy (LE) emission is comparable in energy to that of the 'stair' structures (**55**) or (**58**) but it is at much higher energy than that of the 'chain' (**53b**).

In conclusion, the emissive behavior of (**54**)–(**59**), alone, did not allow a well founded definition of the charge-transfer electronic transitions involved in the second-order NLO response, although a certain sensitivity of the wavelength of the emission to the nature of the halide X would suggest participation of halide-based orbitals to the major charge-transfer process, while inter-metal distances invariably greater than the sum of the van der Waals radii allowed to exclude a $d_{\mathrm{Cu}} \rightarrow (s,p)_{\mathrm{Cu}}$ contribution from Cu-delocalized orbitals. Moreover, the inadequacy of the involvement of a ^{3}MLCT* transition alone emerged from the investigation on the second-order NLO responses via Zyss' model [48]. As a consequence, the charge-transfer process involved in the excited state ^{3}XLCT* appeared as having a possible role in the SHG. This latter assumption was confirmed by the SHG efficiencies of compounds having the same structural motifs and organic ligands but differing for the halides (e.g. compounds (**55**) and (**58**) with SHG of 2.3 and 7.5 times that of quartz, respectively). In addition, we observed that the strength of second-order NLO activities was retraceable to the structure of the polymeric framework. As observed for (**53a**) and (**53b**), 'chains' always show larger second-order NLO efficiencies than 'stairs' (Table 6), suggesting that in the two structural motifs dipole–dipole interactions occur not only through space but also through bonds, in particular within the polymeric framework.

Pursuing the investigation on the emissive and second-order NLO behavior of CuX/L adducts, we have successively reported the results obtained for a series of CuI adducts with some *para*-substituted pyridines and *para*-substituted *trans*-stilbazole [51]. The presence of a bulky *tert*-butyl group in the pyridine stabilizes the tetrameric structure of $[CuI(4\text{-}tert\text{-butylpyridine})]_4$ (**60**) (Fig. 11) with a Cu···Cu non-bonding interaction of 2.72 Å. As expected (**60**) showed in the solid state a broad LE structureless emission, centered at 602 nm [46].

By substitution of the *tert*-butyl group with a less bulky but more electron donor dimethylamino group (**61**), the structural motif changed and resulted in the first example of a hexameric $[CuI(L)]_6$ oligomer (L = *para*-dimethylaminopyridine) (Fig. 12), which could be viewed as a 'cut' portion of a 'stair'. The structural motif of (**61**) was neither reported, nor photophysically studied before, so that its emission, characterized by a low energy maximum at 580 nm, was tentatively attributed, as for all the adducts with a 'stair' polymeric network, to a ^{3}XLCT*

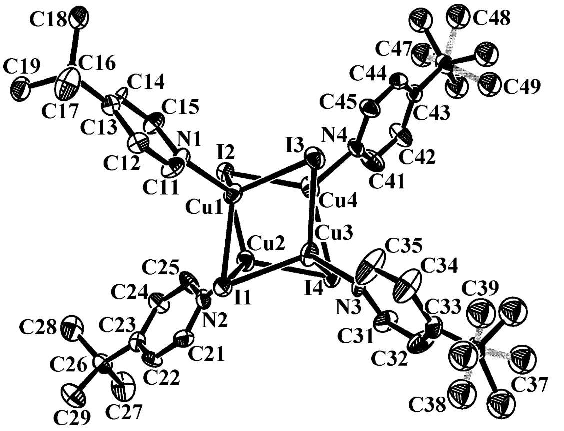

Fig. 11. Representation, with 30% probability Ortep, of the tetrameric structural motif [CuI(4-*tert*-butylpyridine)]$_4$ (**60**) (ref. [51], with copyright permission).

excited state, since the Cu···Cu distance of 2.84 Å, higher then the sum of the van der Waals radii (2.80 Å), allowed discarding any contribution from excited states involving a cluster type metal-delocalized orbitals. However, a ^{3}MLCT* process could not be excluded.

The *trans*-4-stilbazole adduct, [CuI(*trans*-4-stilbazole)]$_n$ (**62**), showed the well known double-stranded 'stair' motif (Fig. 13). On the other side, completely new is the polymeric helicoidal motif of the related adduct [CuI(*trans*-4′-dimethylamino-4-stilbazole)]$_n$ (**63**). Within its asymmetric crystalline unit, each copper coordinates the nitrogen donor atom of one organic ligand, while the iodine atoms simply bridge two metal centers (Fig. 14). In agreement with its non-centrosymmetric crystallization, (**63**) affords a discrete SHG when irradiated at 1.064 μm (with efficiency of 22.5 times that of quartz). The significant change of structural motif on going from (**62**) to (**63**) was suggested as originated by the steric hindrance of the dimethylamino group, which, in the latter compound, prevents the stacking of the ligands on both sides of the CuI skeleton, although electronic factors cannot be discharged taking into consideration the strong electron donor properties of the dimethylamino group.

Rather surprisingly, both (**62**) and (**63**) are not luminescent at room temperature. In (**62**), being a typical 'stair' with a Cu···Cu distance (2.85 Å) higher than the sum of the van der Waals radii, a high energy emission due to ^{3}XLCT* charge-transfer process was expected as it was reported for [CuI(pyridine)]$_n$, [CuI(3-methylpyridine)]$_n$, [CuI(4-methylpyridine)]$_n$ and [CuI(4-acetylpyridine)]$_n$ [47]. Being both the metal and the halide in (**62**) identical to those in the above pyridinic 'stairs' adducts, the presence, in (**62**), of *trans*-stilbazole inevitably drove the attention on the role of π-conjugation extension, since calculations on cofacial stilbenic arrangements have suggested that for intermolecular distances below the critical value of 7 Å, the mixing of HOMO and LUMO orbitals produces excited states characterized by a potentially reduced efficiency of the emission process [52]. In (**62**), the organic *trans*-stilbazole ligands stack at a distance of only 4.15 Å (Fig. 13), but being totally absent the expected ^{3}XLCT* emission typical of a CuI 'stair' structure, the quenching of the emission was suggested to involve both the π systems of *trans*-stilbazoles and the orbitals of the CuI skeleton involved in a non-emissive ^{3}MLCT* charge-transfer process. The involvement of both metal and ligand orbitals in the quenching was suggested also by the solid state emission spectrum of *trans*-stilbazole itself, characterized by a stacking distance of 6.33 Å between the stilbazole molecules which shows an intense emission in the blue spectral region plus a broad and much weaker band in the 500–700 nm region [53].

In the case of (**63**), the quenching process takes place even if the consecutive *trans*-stilbazolic moieties stack at a distance

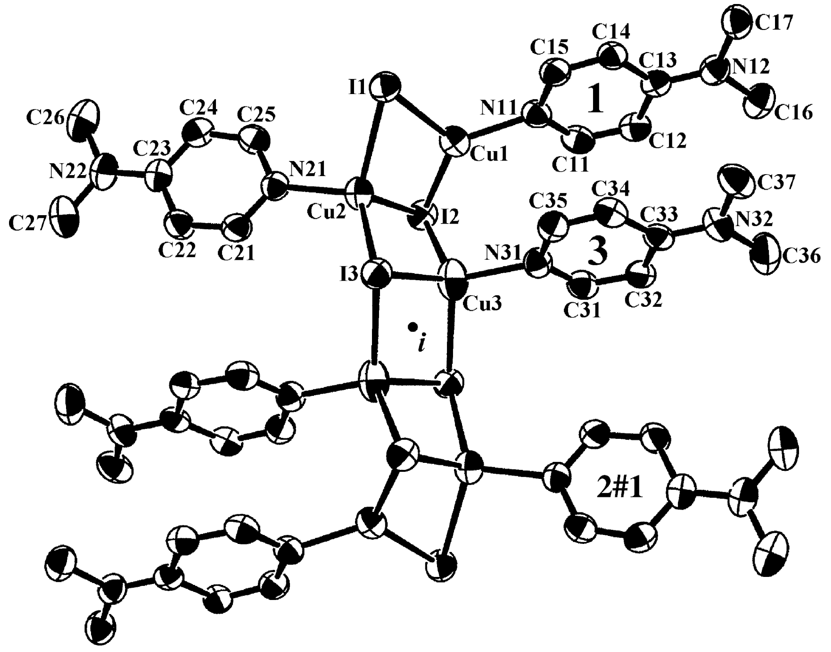

Fig. 12. Representation, with 50% probability Ortep, of the hexameric structural motif in [CuI(4-dimethylaminopyridine)]$_6$ (**61**) (ref. [51], with copyright permission).

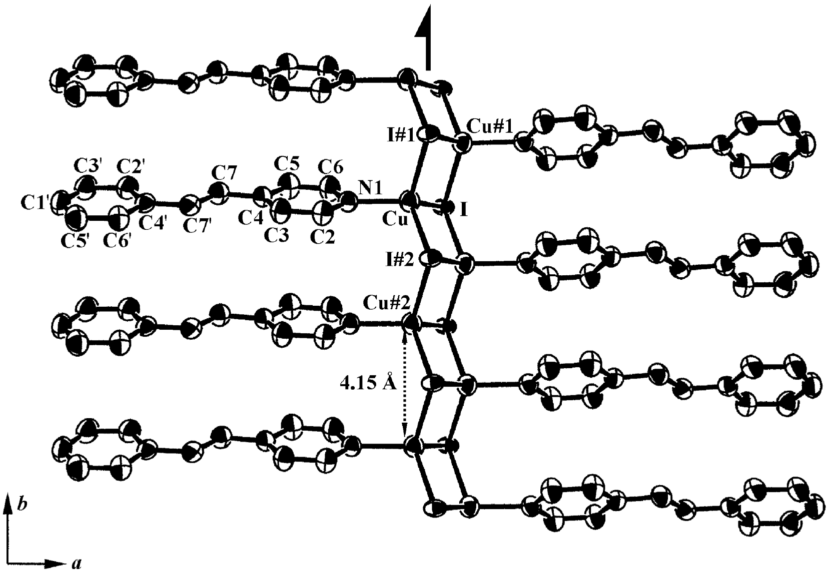

Fig. 13. Representation, with 50% probability Ortep, of the double-stranded 'stair' of compound [CuI(*trans*-4-stilbazole)]$_n$ (**62**) (ref. [51], with copyright permission).

of 7.57 Å above the critical value of 7 Å [52], while crystalline *trans*-4′-dimethylamino-4-stilbazole itself, whose molecules in the crystal structure are stacked at a distance similar to that in (**63**) (7.66 Å) [54] shows two emission peaks at 477 and 503 nm. Therefore, since, as for (**62**), any expected emission attributed to the presence of the CuI polymeric network is completely lacking (based on the rather short Cu···Cu distance, 2.63 Å, an emission due to a charge-transfer process involving the Cu skeleton, would be expected), even for (**63**), the role, in the quenching process, of orbitals belonging to the CuI polymeric skeleton in addition to π orbitals of the *trans*-stilbazolic ligands is probably relevant.

In conclusion, we have not only shown that the 'chain' arrangement of the Cu/halide skeleton produces a higher SHG than the 'stair' arrangement, but also that the extension of the π delocalization in pyridinic ligands may produce quenching of

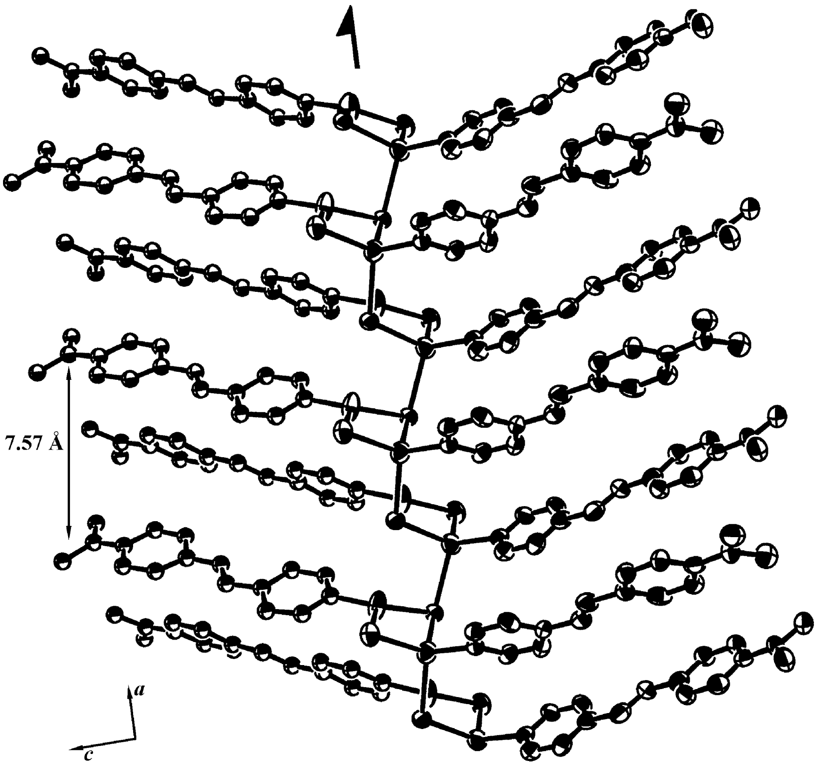

Fig. 14. Representation, with 50% probability Ortep, of the structural motif of compound [CuI(*trans*-4′-dimethylamino-4-stilbazole)]$_n$ (**63**) (ref. [51], with copyright permission).

any emission process, although maintaining a SHG in crystalline asymmetrical structures.

6. Porphyrins as two-dimensional push–pull second-order NLO chromophores

Significant second-order non-linearities in organic molecules arise from one-dimensional highly π delocalized systems [18]. Two-dimensional π delocalized systems like porphyrins, with their extensive two-dimensional 18 π electrons core, have been only recently investigated as third- and second-order NLO molecular materials [55,56] While large part of the investigations have been devoted to the study of third-order NLO properties [56], and in particular to applications for optical limiting [57], our group has been involved, in the last few years, in the less investigated area of the second-order NLO response of asymmetric push–pull porphyrins and their metal complexes.

These latter may be interesting molecular materials since they offer good thermal and chemical stability, acceptable solubility for the determination of molecular properties such as dipole moments and non-linear optical responses and relatively easy synthetic pathways for the preparation of various architectures [58–60] together with potential processability as layers [61].

6.1. The porphyrin ring as a π linker of a push–pull system

The highly polarizable π porphyrin ring, characterized by strong $\pi \rightarrow \pi^*$ transitions [62], has been proposed as a π linker of asymmetrical pseudo-linear push–pull porphyrinic chromophores [63,64a].

However, for asymmetrical tetraarylporphyrins carrying in opposite *meso* positions donor and acceptor groups bound to the *para* positions of the aryl rings, the electronic exchange within the push–pull system and therefore the second-order NLO response was reported to be low both experimentally [64b] and theoretically [65] due to the poor π conjugation between the porphyrin and the phenyl rings, which are not coplanar.

We have confirmed [66], for such kind of asymmetrically substituted chromophores (Fig. 15), a limited second-order NLO response but we have evidenced also a substantial third-order NLO response and therefore we have pointed out that the quadratic hyperpolarizability β, when measured by the EFISH technique, could be also affected by a significant overestimation, because the cubic contribution $\gamma(-2\omega; \omega, \omega, 0)$ to the intrinsic EFISH response γ_{EFISH} cannot be neglected in Eq. (6).

In addition, we have evidenced that in these porphyrins and in their metal complexes, due to their strong absorption bands in the region 0.400–0.650 μm [62], their second-order NLO response must be measured working with a non-resonant incident wavelength of 1.907 μm, because, when working with an incident wavelength of 1.340 μm or even 1.064 μm, the second-order NLO response is affected by relevant resonance enhancements. We reached also experimental evidence that in the porphyrinic push–pull system of Fig. 15 the coordination to a metal ion does not perturb too much the intrinsic γ_{EFISH} response, when working with a non-resonant incident wavelength of 1.907 μm. This result differs from what reported for other π-delocalized macrocycles such as octasubstituted phthalocyanines [67] or triazolohemiporphyrazines [68], but working with an incident wavelength of 1.064 μm. In these latter cases, the dependence of γ_{EFISH} on metal coordination was attributed to a ω resonance enhancement, due to some weak d–d absorptions occurring only in some metal complexes.

Therien and co-workers [69a,b] and Ng and co-workers [69c] have investigated the second-order NLO response of structurally more sophisticated push–pull porphyrinic chromophores such as a 10,20-diphenylporphyrin and its Zn(II) [69a,b], Cu(II) [69a,b] and Ni(II) [69c] complexes, carrying in *meso* 5- and 15-positions, respectively, an electron releasing system (p-$\mathrm{Me_2NC_6H_4{-}C{\equiv}C{-}}$) and a series of different electron-withdrawing systems like p-$\mathrm{NO_2{-}C_6H_4{-}C{\equiv}C{-}}$ [69a] or –CHO, –CH=C(CN)$_2$, –CH=C(COOEt)$_2$, *trans*-CH=CH–CHO [69c]. Due to the planar arrangement of the ring and of the pseudo-linear push–pull system, an effective electron charge-transfer between the donor and acceptor groups by an asymmetric excited state derived from a strong bridge mediated electronic coupling was suggested [63]. In agreement with this latter suggestion an exceptionally high quadratic hyperpolarizability β was reported by Therien and co-workers [69a] for the Cu(II) (**65**) and Zn(II) (**66**) complexes (Fig. 16), measured by Hyper-Raleigh Scattering [69a] working with a probably resonant incident wavelength of 1.064 μm ($\beta_{1.064}$ 1501 × 10^{-30} esu for (**65**) and 4933 × 10^{-30} esu for (**66**), respectively).

In a second time, the value of the quadratic hyperpolarizability, deduced from both absorption and electroabsorption (Stark effect) data [69b], was reported to be lower, although still high (for instance, $\beta_{1.064}$ 1710 × 10^{-30} esu for (**66**), when working with an incident wavelength of 1.064 μm. However, a much lower value of the quadratic hyperpolarizability (around 100 × 10^{-30} esu) was reported later for structurally related

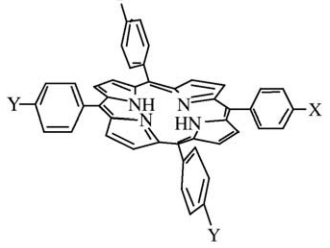

H$_2$**A** X = H Y = H
H$_2$**B** X = NO$_2$ Y = H
H$_2$**C** X = NO$_2$ Y = CH$_3$
H$_2$**D** X = NO$_2$ Y = OCH$_3$

Fig. 15. Asymmetric porphyrins investigated.

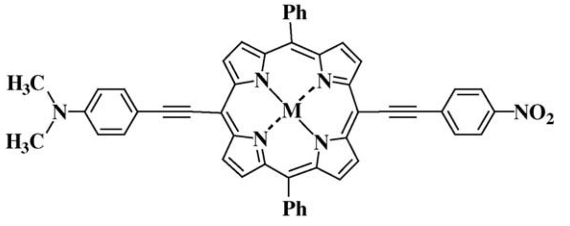

Fig. 16. M = Ni (**64**), Cu (**65**), Zn (**66**).

Ni(II) porphyrinic chromophores, when measured by the EFISH technique working with a non-resonant incident wavelength of 1.907 μm [69c].

Starting from this latter result, we evaluated, by different techniques, the second-order NLO response of the push–pull Ni(II) porphyrinic chromophore (**64**), structurally related to Therien's chromophores (**65**) or (**66**) (Fig. 16), working under similar and well controlled experimental conditions in order to define a consistent value of its quadratic hyperpolarizability. We thus investigated the second-order NLO response of (**64**) using the EFISH technique, working with a non-resonant incident wavelength of 1.907 μm [70]. We have also evaluated the quadratic hyperpolarizability β_{CT} by the solvatochromic method [6] and the static hyperpolarizability β_0 by a vibrational method [71] totally not affected by fluorescence or resonance interferences, which may occur in HRS or EFISH measurements.

The value of the quadratic hyperpolarizability of (**64**) was in all cases consistently much lower (around 80–100 × 10^{-30} esu) than that reported for the corresponding Therien's chromophores (**65**) and (**66**) (see above). In these latter, the large difference cannot be due neither to some strong resonance enhancement of the NLO response due to B or Q absorption bands or to the presence of fluorescent emission, which we have shown to be at much higher wavelength than the second harmonic of an incident wavelength of 1.064 μm [69a]. To confirm these views the quadratic hyperpolarizability of the Therien's chromophore (**66**), obtained from both absorption and electroabsorption data (Stark effect) [67b], was reported to be about 540 × 10^{-30} esu even if working with a non-resonant wavelength of 1.907 μm.

Therefore, we suggested that the quadratic hyperpolarizability of Therien's chromophores like (**64**)–(**66**) may be affected by the nature of the metal, as in some complexes of Schiff bases [1h,72]. Work is actually in progress in our laboratory both experimentally and theoretically in order to define the real origin of such a large difference.

6.2. The porphyrin ring as an ambivalent donor or acceptor group of a push–pull system

The investigation of the second-order NLO properties of the porphyrin ring in a push–pull system can not only be limited to its role as a highly polarizable π linker of an extended pseudo-linear push–pull system, but also to its intrinsic donor or acceptor properties as defined in an interesting paper of Ratner, Marks and co-workers [65]. Stimulated by this latter work we have investigated if the π system of porphyrins or metalloporphyrins may act as a donor or acceptor group of a pseudo linear push–pull chromophore. Depending on the number of π electrons, π orbitals and on the heteroatom electronegativities, heterocyclic rings can act as electron excessive (donor) or electron deficient (acceptor) systems [73]. Pyrrole with six π electrons and five π orbitals is an electron excessive π system. Thus, the porphyrinic chromophore with four pyrrole rings may act as a π electron excessive system, in which electron excessive carbon atoms such as β pyrrolic atoms may be identified [65]. We have thus investigated the second-order NLO response of push–pull pseudo linear chromophores based on a 5,10,15,20-tetraphenylporphyrin, either as free base or as Zn(II) complexes, carrying a push or a pull group linked to β pyrrolic position, through a π delocalized linker (Fig. 17) [57].

In order to avoid resonance enhancements, their second-order NLO response was measured by the EFISH technique working with a non-resonant 1.907 μm incident wavelength. Calculations based on the Density Functional Theory (DFT) [74] have been also carried out in order to define the best structural geometries using the BP86 functional [75] and an all-electron valence triple-ξ basis set with polarization functions on all atoms [76]. These calculations have evidenced a nearly planar arrangement of the porphyrin ring and of all the π linkers (either ethylenic or acethylenic) carrying the donor or acceptor group, thus producing a nearly planar chromophore characterized by facile π interaction between the β carbon atom of the porphyrin ring and the π linker. Evidence for such a π interaction, which perturbs the microsymmetry of the π porphyrin system, was deduced for chromophores carrying an electron-withdrawing NO_2 group from the asymmetry of the B Soret band, the increase of its bandwidth and the strong perturbation of the center of gravity of B and Q_α bands [59].

Such π interaction between the porphyrin ring and the π system of the linker is the origin of some charge-transfer character of both B and Q bands, as shown by a solvatochromic investigation, which suggests that B and Q transitions are not anymore

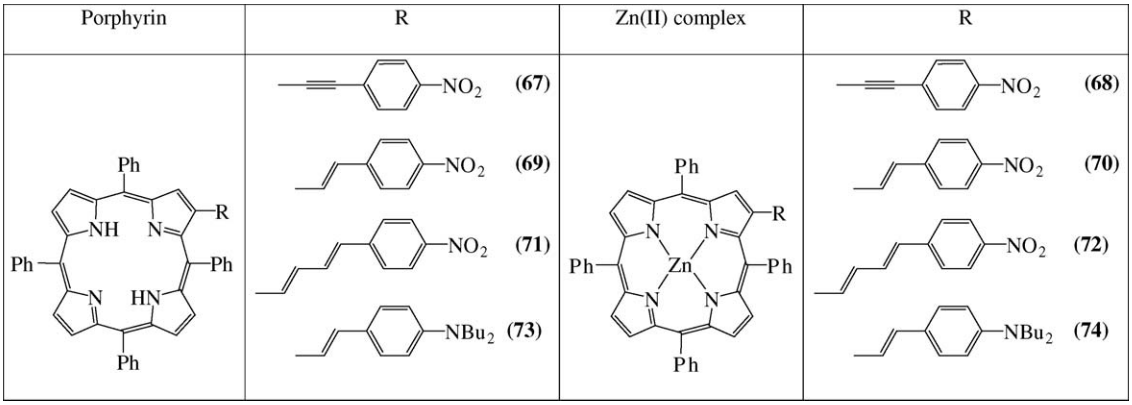

Fig. 17. Asymmetric tetraphenyl porphyrins and their Zn(II) complexes with electron donor or electron-withdrawing substituents in β pyrrolic position investigated in ref. [57].

Table 7
Experimental and theoretical dipole moments and EFISH $\beta_{1.907}$ in $CHCl_3$ solution of various porphyrins and their Zn(II) complexes

Molecule[a]	μ_{exp} (μ_{theor}) (D)	$\beta_{1.91}$ (10^{-30}esu)[b]
2-(4-Nitrophenyl)ethinyl-H_2TPP (**67**)	6.1 (8.55)[c]	30.1[d]
2-(4-Nitrophenyl)ethinyl-ZnTPP (**68**)	7.1 (8.82)	20.4[d]
trans-2-(4-Nitrophenyl)ethenyl-H_2TPP (**69**)	6.6 (8.31)[c]	39.3[d]
trans-[2-(4-Nitrophenyl)ethenyl-ZnTPP (**70**)	7.0 (8.69)	29.7[d]
trans,*trans*-2-(4-Nitrophenyl)buta-1,3-dienyl-H_2TPP (**71**)	6.2 (9.30)[c]	42.8[d]
trans,*trans*-[2-(4-Nitrophenyl)buta-1,3-dienyl-ZnTPP (**72**)	7.1 (9.46)	43.1[d]
trans-2-[4-(Dibutylamino)phenyl]ethenyl-H_2TPP (**73**)	(5.33)[c,e]	75.7[d,f]
trans-2-[4-(Dibutylamino)phenyl]ethenyl-ZnTPP (**74**)	(5.16)[e]	127.5[d,f]

[a] H_2TPP means 5,10,15,20-tetraphenylporphyrin.
[b] Obtained by Eq. (6) (see text) omitting the cubic contribution $\gamma(-2\omega; \omega, \omega, 0)$.
[c] The theoretical value is the semisum of the theoretical dipole moments of two isomeric structures.
[d] The error is about ±10–15%.
[e] Theoretical value calculated by an ab initio approach.
[f] Using theoretical dipole moment.

centered only on the porphyrin ring. Therefore, the π electronic system is asymmetric and involves also the π orbitals of the linker [59].

This asymmetry was also confirmed by the significant values of dipole moments (either measured experimentally or calculated theoretically) and by the inversion of the polarity when the electron-withdrawing nitro group is substituted by the electron donor dibutylamino group (Table 7).

Therefore, already in the ground state the porphyrin ring, substituted in β pyrrolic position, shows thus an ambivalent char-

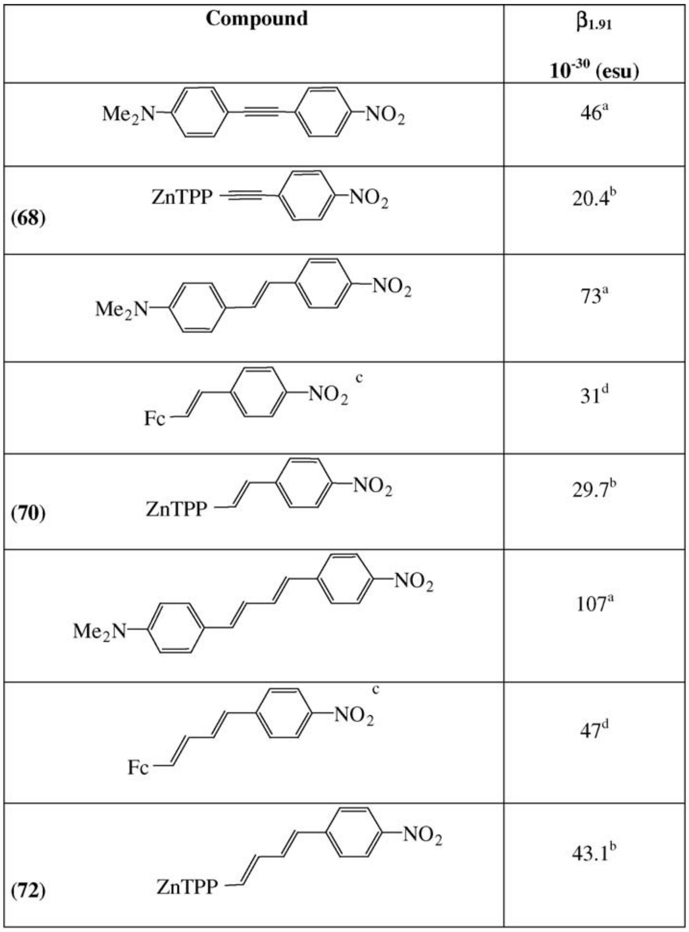

(a) Ref. [18a]; (b) Ref. [59]; (c) Fc = ferrocene; (d) Ref. [78]; H_2TPP means 5,10,15,20 tetraphenylporphyrin

Fig. 18. Quadratic hyperpolarizability ($\beta_{1.91}$) of some organic and organometallic push–pull systems, measured in $CHCl_3$ by the EFISH technique at an incident wavelength of 1.91 μm. (a) Ref. [18a]; (b) ref. [59]; (c) Fc = ferrocene; (d) ref. [78]; H_2TPP means 5,10,15,20-tetraphenylporphyrin.

acter, acting as acceptor, according to the presence of an electron donor or an electron-withdrawing group connected through the π linker [59].

We suggested that the charge-transfer process involving the porphyrin π core and the π orbitals of the linker is probably the origin of the quadratic hyperpolarizability of these chromophores when carrying a nitro group (Table 7), as in classical 1D push–pull organometallic [8,15] and organic chromophores [18]. In chromophores (**67**)–(**72**), the porphyrin ring acts as a donor push group comparable as strength to the ferrocenyl group but slightly lower than the 4-dimethylaminophenyl group (Fig. 18).

Unexpectedly, chromophores (**73**) and (**74**), carrying a dibutylamino group, show a higher and still positive quadratic hyperpolarizability (Table 7). The lack of bandwidth increase of the B band, its symmetry and the lower perturbation of the centere of gravity of B and Q_α bands for both (**73**) and (**74**) do not support an excitation process involving a significant charge-transfer from the π porphyrin core to the π linker, as suggested for chromophores (**67**)–(**72**). Moreover, if this charge-transfer is the origin of the second-order NLO response, the quadratic hyperpolarizability should be negative. The significant positive values of the quadratic hyperpolarizability of (**73**) and (**74**) were tentatively attributed to an effective screening of the ground state polarization induced by the electron rich β pyrrolic position of the porphyrin ring, which thus behaves as an acceptor increasing, in the $n \rightarrow \pi^*$ excitation process, the donor properties of the dibutylamino push group connected by the π linker.

Although this latter hypothesis must be still proved, for instance, by a TD-DFT theoretical approach, which is under way in our laboratory, we have experimentally proved with our work that the porphyrin ring, through its β pyrrolic carbon atom, can show an ambivalent donor–acceptor character both in the ground state and in processes involving excited states like the second-order NLO response. We are actually extending this kind of investigation to 10,20-diphenylporphyrins and their Zn(II) complexes bound in the *meso* position to a π delocalized linker (either ethylenic or acetylenic) carrying an electron-withdrawing nitro or an electron donor dibutylamino group in the *para* position of the phenyl ring [77].

7. Conclusion

In our series of investigations, we have clearly shown that by interaction with a metal center we have a flexible way to tune the second-order NLO response of organic push–pull second-order NLO chromophores acting as ligands.

Through the modulation of the nature and the oxidation state of the metal and its coordination sphere through ancillary ligands or chelation, such response can be not only increased, sometimes in a very significant way, but also its sign can be changed.

We think that our investigations have produced now enough information to help the research aimed to the design of improved new second-order NLO organometallic or coordination chromophores.

We have also shown that push–pull 1D chromophores with organometallic or coordination moieties as push or pull groups, structurally similar to classical push–pull 1D organic chromophores, behave in a different way from these latter. In fact, the charge-transfer process controlling their second-order NLO response remains located around the donor organometallic push group without a complete charge-transfer from the push to pull groups as it occurs on the contrary in classical organic 1D push–pull chromophores. Our recent work on the more complex 2D chromophores, based on porphyrins and their metal complexes, is in a relatively new field of research, quite difficult both for the increasing synthetic complexity and for the limited knowledge of the rules controlling the molecular design and for the difficult understanding of the polarization processes involving excitation processes in these large π delocalized chromophores.

Finally, we recently have synthesized and characterized some new hybrid inorganic–organic crystalline materials with high SHG and we are actually investigating the origin of the self organization processes of the organic chromophores occurring during crystallization of these hybrid materials and also the role of a polymeric network involving metals in defining the second-order NLO responses of some Cu(I) adducts. The understanding of processes controlling and favouring the ordered organization of organic or organometallic chromophores within an inorganic or polymeric network to produce bulk materials with improved NLO properties is one of the main objectives of our research group in the next years. We plan also to study new organometallic or coordination chromophores with some specific third-order NLO properties such as two photon absorption (TPA).

In conclusion, there is a lot of room for new and enjoying chemistry in the field of new materials for photonic and electrooptical applications.

Acknowledgments

This work was supported by the Ministero dell'Università e della Ricerca Scientifica e Tecnologica (Programma di Ricerca di tipo Interuniversitario nell'area delle scienze chimiche, year 1997, Research Title: Molecole per materiali Funzionali Nanostrutturati and year 2001, Research Title: Nanotecnologie Molecolari per Materiali Magnetici e per Ottica Non-Lineare); by the Ministero dell'Istruzione, dell'Università e della Ricerca (Programma di ricerca FIRB, year 2001, Research Title: Nano-organization of hybrid organo-inorganic molecules with magnetic and non-linear optical properties; Programma di ricerca FISR, year 2001, Research Title: Nanotecnologie molecolari per l'immagazzinamento e la trasmissione delle informazioni); by the Consiglio Nazionale delle Ricerche (Progetto Finalizzato Materiali Speciali per Tecnologie avanzate II 1998. Research Title: Sintesi e sviluppo di composti molecolari organometallici e di coordinazione con proprietà di ottica non-lineare (NLO) e con proprietà elettriche anisotropiche e isotropiche). We deeply thank Prof. J. Zyss and Prof. I. Ledoux-Rak (Ecole Normale Supérieure de Cachan, France), Prof. P.C. Ford (University of California, Santa Barbara, USA), and Dr. V. Srdanov (IQUEST, Santa Barbara, California, USA) for their qualified suggestions and for helping us in getting in the field of linear and non-linear optics and the Italian research groups of Prof. F. Cariati and Prof. S. Bruni, (Milan University), Prof. P.C. Fantucci (Milano Bicocca University), Prof. P. Mussini (Milan University), Dr. S. Quici (Milan ISTM-CNR), Prof. A. Sgamelotti (Perugia University and ISTM-CNR), Prof. A. Sironi (Milan University), and Prof. G. Zerbi (Politecnico di Milano) for helpful discussions and scientific collaboration.

References

[1] (a) H.S. Nalwa, Appl. Organomet. Chem. 5 (1991) 349;
  (b) J. Zyss, Molecular Nonlinear Optics, Academic Press, New York, 1994;
  (c) N.J. Long, Angew Chem. Int. Ed. Engl. 34 (1995) 21;
  (d) J. Heck, S. Dabek, T. Meyer-Friedrichsen, H. Wong, Coord. Chem. Rev. 190–192 (1999) 1217;
  (e) D.M. Roundhill, J.P. Fackler, Optoelectronic Properties of Inorganic Compounds, Plenum Press, New York, 1999;
  (f) J. Heck, S. Dabek, T. Meyer-Friedrichsen, H. Wong, Coord. Chem. Rev. 190–192 (1999) 1217;
  (g) H. Le Bozec, T. Renouard, Eur. J. Inorg. Chem. (2000) 229;
  (h) P.G. Lacroix, Eur. J. Inorg. Chem. (2001) 339;
  (i) S. Di Bella, Chem. Soc. Rev. 30 (2001) 355;
  (j) B.J. Coe, in: J.A. McCleverty, T.J. Meyer (Eds.), Comprehensive Coordination Chemistry II, vol. 9, Elsevier Pergamon, Oxford, UK, 2004, pp. 621–687;
  (k) B.J. Coe, N.R.M. Curati, Comments Inorg. Chem. 25 (2004) 147.
[2] (a) J.L. Oudar, D.S. Chemla, J. Chem. Phys. 66 (1977) 2664;
  (b) J.L. Oudar, J. Chem. Phys. 67 (1977) 446;
  (c) J.L. Oudar, H. Le Person, Opt. Commun. 15 (1975) 258.
[3] (a) J. Zyss, I. Ledoux, Chem. Rev. 94 (1994) 77;
  (b) H. Le Bozec, T. Le Boudere, O. Maury, I. Ledoux, J. Zyss, J. Opt. A: Pure Appl. Opt. 4 (2002) 5189.
[4] (a) B.F. Levine, C.G. Bethea, Appl. Phys. Lett. 24 (1974) 445;
  (b) K.D. Singer, A.F. Garito, J. Chem. Phys. 75 (1981) 3572;
  (c) I. Ledoux, J. Zyss, Chem. Phys. 73 (1982) 203.
[5] (a) R.W. Terhune, P.D. Maker, C.M. Savage, Phys. Rev. Lett. 14 (1965) 681;
  (b) P.D. Maker, Phys. Rev. 1 (1970) 923;
  (c) K. Clays, A. Pearson, Phys. Rev. Lett. 66 (1991) 2980.
[6] (a) E.G. Mc Rae, J. Phys. Chem. 61 (1957) 562;
  (b) S. Bruni, F. Cariati, E. Cariati, F.A. Porta, S. Quici, D. Roberto, Spectrochim. Acta Part A 57 (2001) 1417.
[7] S.K. Kurtz, T.J. Perry, J. Appl. Phys. 39 (1968) 3798.
[8] D. Roberto, R. Ugo, S. Bruni, E. Cariati, F. Cariati, P.C. Fantucci, I. Invernizzi, S. Quici, I. Ledoux, J. Zyss, Organometallics 19 (2000) 1775.
[9] D. Roberto, R. Ugo, F. Tessore, E. Lucenti, S. Quici, S. Vezza, P.C. Fantucci, I. Invernizzi, S. Bruni, I. Ledoux-Rak, J. Zyss, Organometallics 21 (2002) 161.
[10] F. Tessore, D. Roberto, R. Ugo, P. Mussini, S. Quici, I. Ledoux-Rak, J. Zyss, Angew Chem. 115 (2003) 472;
  F. Tessore, D. Roberto, R. Ugo, P. Mussini, S. Quici, I. Ledoux-Rak, J. Zyss, Angew Chem. Int. Ed. Engl. 42 (2003) 456.
[11] F. Tessore, D. Locatelli, S. Righetto, D. Roberto, R. Ugo, P. Mussini, Inorg. Chem. 44 (2005) 2437.
[12] D. Roberto, F. Tessore, R. Ugo, S. Bruni, A. Manfredi, S. Quici, Chem. Commun. (2002) 846.
[13] F. De Angelis, S. Fantacci, A. Sgamelotti, F. Cariati, D. Roberto, F. Tessore, R. Ugo, J. Chem. Soc. Dalton Trans. (2005) in press.
[14] B.J. Orr, J.F. Ward, Mol. Phys. 20 (1971) 513.
[15] D.R. Kanis, P.G. Lacroix, M.A. Ratner, T.J. Marks, J. Am. Chem. Soc. 116 (1994) 10089.
[16] (a) L.T. Cheng, W. Tam, G.R. Meredith, S.R. Marder, Mol. Cryst. Liq. Cryst. 189 (1990) 137;
  (b) L.T. Cheng, W. Tam, D.F. Eaton, Organometallics 9 (1990) 2856.
[17] (a) J. Zyss, J. Non-Cryst. Solids 47 (1982) 211;
  (b) D.J. Williams, Angew Chem. Int. Ed. Engl. 23 (1984) 690;
  (c) G.R. Meredith, Mater. Res. Bull., August (1988) 24;
  (d) S. Tripathy, E. Cavicchi, J. Kumar, R.S. Kumar, Chemtech 19 (1989) 620;
  (e) S.R. Marder, J.W. Perry, C.P. Yakymyshyn, Chem. Mater. 6 (1994) 1137;
  (f) D.M. Burland, Chem. Rev. 94 (1994) 1.
[18] (a) L.T. Cheng, W. Tam, S.H. Stevenson, G.R. Meredith, G. Rikken, S.R. Marder, J. Phys. Chem. 95 (1991) 10631;
  (b) L.T. Cheng, W. Tam, S.R. Marder, A.E. Stiegman, G. Rikken, C.W. Spangler, J. Phys. Chem. 95 (1991) 10643.
[19] K.D. Singer, E. Sohn, L.A. King, H.M. Gordon, H.E. Katz, P.W. Dirk, J. Opt. Soc. Am. B 6 (1989) 1339.
[20] E. Lucenti, E. Cariati, C. Dragonetti, L. Manassero, F. Tessore, Organometallics 23 (2004) 687.
[21] (a) M. Bourgault, C. Mountassir, H. Le Bozec, I. Ledoux, G. Pucetti, J. Zyss, J. Chem. Soc. Chem. Commun. (1993) 1623;
  (b) M. Bourgault, K. Baum, H. Le Bozec, G. Pucetti, I. Ledoux, J. Zyss, N. J. Chem. (1998) 517.
[22] A. Hilton, T. Renouard, O. Maury, H. Le Bozec, I. Ledoux, J. Zyss, Chem. Commun. (1999) 2521.
[23] (a) J. Collin, I.M. Dixon, J. Sauvage, J.A.G. Williams, F. Barigelletti, L. Flamigni, J. Am. Chem. Soc. 121 (1999) 5009;
  (b) F. Neve, A. Crispini, F. Loiseau, S. Campagna, J. Chem. Soc. Dalton Trans. (2000) 1399.
[24] (a) D.D. Walker, H. Taube, Inorg. Chem. 20 (1981) 2828;
  (b) J.C. Curtis, B.P. Sullivan, T.J. Meyer, Inorg. Chem. 22 (1983) 224.
[25] K. Kalyanasundaram, S.M. Zakeeruddin, K. Nazeeruddin, Coord. Chem. Rev. 132 (1994) 259.
[26] M. Pizzotti, R. Ugo, D. Roberto, S. Bruni, P.C. Fantucci, C. Rovizzi, Organometallics 21 (2002) 5830.
[27] M.J.G. Lesley, A. Woodward, N.J. Taylor, T.B. Marder, I. Cazenobe, I. Ledoux, J. Zyss, A. Thornton, D.W. Bruce, A.K. Kakkar, Chem. Mater. 10 (1998) 1355.
[28] M.M. Zulu, A.J. Lees, Organometallics 8 (1989) 955.
[29] M. Bruschi, P.C. Fantucci, M. Pizzotti, J. Phys. Chem. 109 (2005) 9637.
[30] M. Pizzotti, R. Ugo, C. Dragonetti, E. Annoni, F. Demartin, P. Mussini, Organometallics 22 (2003) 4001.
[31] (a) D.S. Chemla, J. Zyss (Eds.), Nonlinear Optical Properties of Organic Molecules and Crystals, vol. 1, Academic Press, Orlando, FL, 1987;
  (b) J. Zyss (Ed.), Molecular Nonlinear Optics: Materials, Physics and Devices, Academic Press, New York, 1994.
[32] G.R. Meredith, in: J.D. Williams (Ed.), ACS Symposium Series, vol. 233, American Chemical Society, Washington, DC, 1983, pp. 27–56.
[33] (a) P.G. Lacroix, A.V. Veret Lemarinier, R. Clément, K. Nakatani, J.A. Delaire, J. Mater. Chem. 3 (1993) 499;
  (b) P.G. Lacroix, R. Clément, K. Nakatani, J.A. Delaire, J. Zyss, I. Ledoux, Science 263 (1994) 658;
  (c) T. Corradin, R. Clemÿnt, P.G. Lacroix, K. Nakatani, Chem. Mater. 8 (1996) 2153.
[34] T. Yi, R. Clément, C. Haut, L. Catala, T. Gacoin, N. Tancrez, I. Ledoux, J. Zyss, Adv. Mater. 17 (2005) 335.
[35] S. Bénard, P. Yu, J.P. Audière, E. Rivière, R. Clément, J. Guilhem, L. Tchertanov, K. Nakatani, J. Am. Chem. Soc. 122 (2000) 9444.
[36] A.M. Guloy, Z. Tang, P.B. Miranda, V.I. Srdanov, Adv. Mater. 13 (2001) 833.
[37] E. Cariati, R. Ugo, F. Cariati, D. Roberto, N. Masciocchi, S. Galli, A. Sironi, Adv. Mater. 13 (2001) 1665.
[38] N. Masciocchi, A. Sironi, J. Chem. Soc. Dalton Trans. (1997) 4643.
[39] D. Mobius, Adv. Mater. 7 (1995) 437.
[40] P.C. Ford, E. Cariati, J. Bourassa, Chem. Rev. 99 (1999) 3625 (and references therein).

[41] The reader is directed to, for example;
(a) P.C. Healy, C. Pakawatchai, A.H. White, J. Chem. Soc. Dalton Trans. (1983) 1917;
(b) J.C. Dyason, P.C. Healy, C. Pakawatchai, V.A. Patrick, A.H. White, Inorg. Chem. 24 (1985) 1957;
(c) J.C. Dyason, L.M. Engelhardt, P.C. Healy, J.C. Kildea, A.H. White, Aust. J. Chem. 41 (1988) 335;
(d) M.J. Jedrzejas, R.A. Martuch, R.L.R. Towns, R.J. Baker, S.A. Duraj, S.F. Hepp, Acta Crystallogr. Sect. C (Cr. Str. Commun.) 49 (1993) 536.

[42] The reader can refer to, for example;
(a) P.C. Healy, C. Pakawatchai, A.H. White, J. Chem. Soc. Dalton Trans. (1983) 1917;
(b) J.C. Dyason, L.M. Engelhardt, P.C. Healy, A.H. White, Aust. J. Chem. 37 (1984) 2201;
(c) V. Scramm, A. Pierre, W. Hiller, Acta Crystallogr. Sect. C (Cr. Str. Commun.) 40 (1984) 1840;
(d) W. Hiller, Z. Naturforsh. Teil B 39 (1984) 861;
(e) J.C. Dyason, L.M. Engelhardt, P.C. Healy, C. Pakawatchai, A.H. White, Inorg. Chem. 24 (1985) 1950;
(f) M.W. Fuller, V. Costanzo, K.S. Murray, D. St, C. Black, T.W. Hambley, M.R. Snow, Aust. J. Chem. 38 (1985) 865;
(g) J.C. Dyason, L.M. Engelhardt, P.C. Healy, C. Pakawatchai, A.H. White, Inorg. Chem. 24 (1985) 1950;
(h) N.P. Rath, J.L. Maxwell, E.M. Holt, J. Chem. Soc. Dalton Trans. (1986) 2449;
(i) P.C. Healy, J.D. Kildea, B.W. Skelton, A.F. Waters, A.H. White, Acta Crystallogr. Sect. C (Cr. Str. Commun.) 47 (1991) 1721.

[43] The reader is directed to, for example;
(a) C.L. Raston, A.H. White, J. Chem. Soc. Dalton Trans. (1976) 2153;
(b) V. Schramm, Cryst. Struct. Commun. 9 (1980) 1231;
(c) M.R. Churchill, G. Davies, M.A. El-Sayed, J.P. Hutchinson, M.W. Rupich, Inorg. Chem. 21 (1982) 995;
(d) J.C. Dyason, P.C. Healy, L.M. Engelhardt, C. Pakawatchai, V.A. Patrick, C.L. Raston, A.H. White, J. Chem. Soc. Dalton Trans. (1985) 831;
(e) P.C. Healy, C. Pakawatchai, C.L. Raston, B.W. Skelton, A.H. White, J. Chem. Soc. Dalton Trans. (1983) 1905;
(f) L.M. Engelhardt, P.C. Healy, J.D. Kildea, A.H. White, Aust. J. Chem. 42 (1989) 107;
(g) E. Sugahara, M.M.S. Paula, I. Vencato, C.V. Franco, J. Coord. Chem. 39 (1996) 59.

[44] The reader can refer to, for example;
(a) J.A. Campbell, C.L. Raston, A.H. White, Aust. J. Chem. 30 (1977) 1937, The reader can refer to, for example;
(b) P.C. Pakawatchai, C.L. Raston, B.W. Skelton, A.H. White, J. Chem. Soc. Dalton Trans. (19831905);
(c) P.C. Healy, J.D. Kildea, B.W. Skelton, A.H. White, Aust. J. Chem. 42 (1989) 115;
(d) L.M. Engelhardt, P.C. Healy, J.D. Kildea, B.W. Skelton, A.H. White, Aust. J. Chem. 42 (1989) 933.

[45] The reader is directed to, for example;
(a) J.A. Campbell, C.L. Raston, A.H. White, Aust. J. Chem. 30 (1977) 1937;
(b) E. Eitel, D. Oelkrug, W. Hiller, J. Strahle, Z. Naturforsh. Teil B 35 (1980) 1247;
(c) N.P. Rath, J.L. Maxwell, E.M. Holt, J. Chem. Soc. Dalton Trans. (1986) 2449;
(d) P.C. Healy, J.D. Kildea, B.W. Skelton, A.H. White, Aust. J. Chem. 42 (1989) 93;
(e) L.M. Engelhardt, P.C. Healy, J.D. Kildea, A.H. White, Aust. J. Chem. 42 (1989) 185;
(f) P.C. Healy, B.W. Skelton, F. Waters, A.H. White, Aust. J. Chem. 44 (1991) 1049.

[46] (a) K.R. Kyle, C.K. Ryu, J. DiBenedetto, P.C. Ford, J. Am. Chem. Soc. 113 (1991) 2954;
(b) M. Vitale, W.E. Palke, P.C. Ford, J. Phys. Chem. 96 (1992) 8329.

[47] E. Cariati, B. Xianhui, P.C. Ford, Chem. Mater. 12 (2000) 3385.

[48] E. Cariati, D. Roberto, R. Ugo, P.C. Ford, S. Galli, A. Sironi, Chem. Mater. 14 (2002) 5116.

[49] M.A.S. Goher, T.C.W. Mak, Inorg. Chim. Acta 127 (1987) L13.

[50] (a) J. Zyss, J.L. Oudar, Phys. Rev. A 26 (1982) 2028;
(b) J. Zyss, D.S. Chemla, in: D.S. Chemla, J. Zyss (Eds.), Nonlinear Optical Properties of Organic Molecules and Crystals, vol. 1, Academic Press Inc., Orlando, FL, 1987, pp. 23–187.

[51] E. Cariati, D. Roberto, R. Ugo, P.C. Ford, S. Galli, A. Sironi, Inorg. Chem. 44 (2005) 4077.

[52] J. Cornil, D.A. dos Santos, X. Crispin, R. Silbey, J.L. Bredas, J. Am. Chem. Soc. 120 (1998) 1289.

[53] E. Cariati, D. Roberto, R. Ugo, V.I. Srdanov, S. Galli, P. Macchi, A. Sironi, N. J. Chem. 26 (2002) 13.

[54] P.G. Lacroix, J.C. Daran, K. Nakatani, Chem. Mater. 10 (1998) 1109.

[55] G. de la Torre, P. Vazquez, F. Agullo-Lopez, T. Torres, Chem. Rev. 104 (2004) 3723 (and references therein).

[56] (a) S.M. Kuebler, R.G. Denning, H.L. Anderson, J. Am. Chem. Soc. 122 (2000) 339;
(b) M. Drobizhev, A. Karotki, M. Kruk, N.Z.h. Mamardashvili, A. Rebane, Chem. Phys. Lett. 361 (2002) 504.

[57] (a) M. Calvete, G.Y. Yang, M. Hanack, Synthetic Metals 141 (2004) 231 (and references therein);
(b) R.B. Martin, H. Li, L. Gu, S. Kumar, C.M. Sanders, Y.P. Sun, Optical Mater. 27 (2005) 1340.

[58] J.S. Lindsey, in: F. Montanari, L. Casella (Eds.), Metalloporphyrins Catalysed Oxidations, Kluwer Acad. Publ., 1994, p. 49 (and references therein).

[59] E. Annoni, M. Pizzotti, R. Ugo, S. Quici, T. Morotti, M. Bruschi, P. Mussini, Eur. J. Inorg. Chem. (2005) 0000.

[60] T.E.O. Screen, I.M. Blake, L.H. Rees, W. Clegg, S.J. Borwick, H.L. Anderson, J. Chem. Soc. Perkin Trans. I (2002) 320 (and references therein).

[61] D.A. Offord, S.B. Sachs, M.S. Ennis, T.A. Eberspacher, J.H. Griffin, C.E.D. Chidsey, J.P. Collman, J. Am. Chem. Soc. 120 (1998) 4478 (and references therein).

[62] M. Gouterman, in: D. Dolphin (Ed.), The Porphyrins, vol. III, Academic Press, New York, 1978.

[63] S. Priyadarshy, M.J. Therien, D.N. Beratan, J. Am. Chem. Soc. 118 (1996) 1504.

[64] (a) H. Chou, K.S. Suslick, J. Phys. Chem. 98 (1994) 383;
(b) K.S. Suslick, C.T. Chen, G.R. Meredith, L.T. Cheng, J. Am. Chem. Soc. 114 (1992) 6928.

[65] I.D.L. Albert, T.J. Marks, M.A. Ratner, Chem. Mater. 10 (1998) 753.

[66] M. Pizzotti, R. Ugo, E. Annoni, S. Quici, I. Ledoux-Rak, G. Zerbi, M. Del Zoppo, P. Fantucci, I. Invernizzi, Inorg. Chim. Acta 340 (2002) 70 (and references therein about the EFISH technique).

[67] M.A. Dìaz-Garcìa, I. Ledoux, J.A. Duro, T. Torres, F. Agullò-Lòpez, J. Zyss, J. Phys. Chem. 98 (1994) 8761.

[68] M.A. Dìaz-Garcìa, I. Ledoux, F. Fernàndez-Làzaro, A. Sastre, T. Torres, F. Agullò-Lòpez, J. Zyss, J. Phys. Chem. 98 (1994) 4495.

[69] (a) S.M. Le Cours, H.W. Guan, S.G. Di Magno, C.H. Wang, M.J. Therien, J. Am. Chem. Soc. 118 (1996) 1497;
(b) L. Karki, F.W. Vance, J.H. Hupp, S.M. Le Cours, M.J. Therien, J. Am. Chem. Soc. 120 (1998) 2606;
(c) M. Yeung, A.C.H. Ng, M.G.B. Drew, E. Vorpagel, E.M. Breitung, R.J. McMahon, D.K.P. Ng, J. Org. Chem. 63 (1998) 7143.

[70] M. Pizzotti, E. Annoni, R. Ugo, S. Bruni, S. Quici, P. Fantucci, M. Bruschi, G. Zerbi, M. Del Zoppo, J. Porphyrins Phtalocyanines 8 (2004) 1311.

[71] (a) C. Castiglioni, M. Gussoni, M. Del Zoppo, G. Zerbi, Solid State Comm. 82 (1992) 13;
(b) M. Del Zoppo, C. Castiglioni, G. Zerbi, Nonlinear Opt. 9 (1995) 73.

[72] (a) S. Di Bella, I. Fragalà, I. Ledoux, T.J. Marks, J. Am. Chem. Soc. 117 (1995) 9481;

(b) S. Di Bella, I. Fragalà, I. Ledoux, M.A. Dìaz-Garcìa, T.J. Marks, J. Am. Chem. Soc. 119 (1997) 9550.

[73] P.R. Varanasi, A.K.-Y. Jen, J. Chandrasekhar, I.N.N. Namboothiri, A. Rathna, J. Am. Chem. Soc. 188 (1996) 12443.

[74] (a) A.D. Becke, J. Chem. Phys. 98 (1993) 5648;
(b) C. Lee, W. Yang, R.G. Parr, Phys. Rev. 37 (1998) 785.

[75] (a) A.D. Becke, Phys. Rev. A 38 (1988) 3098;
(b) J.P. Perdew, Phys. Rev. B33 (1986) 8822.

[76] A. Schafer, C. Huber, R. Ahlrichs, J. Chem. Phys. 100 (1994) 5829.

[77] T. Morotti, M. Pizzotti, R. Ugo, S. Quici, M. Bruschi, P. Mussini, S. Righetto, Eur. J. Inorg. Chem., submitted for publication.

[78] D.R. Kanis, M.A. Ratner, T.J. Marks, J. Am. Chem. Soc. 114 (1992) 10338 (and references therein).